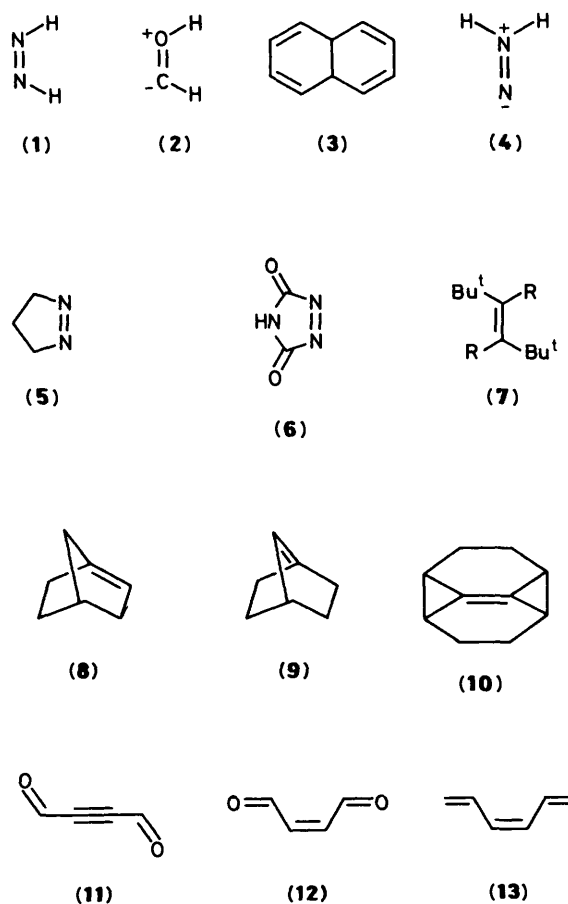


A Theoretical MNDO and AM1 SCF-MO Study of Dihydrogen Transfer Reactions

Dimitris K. Agrafiotis and Henry S. Rzepa*
 Department of Chemistry, Imperial College, London, SW7 2AY

The mechanisms of concerted and stepwise dihydrogen transfer reactions have been studied for a wide variety of hydrogen donors and acceptors using the MNDO and AM1 semiempirical SCF-MO methods. The calculated barriers for concerted [1,2]dihydrogen transfer from *cis*-di-imide were sensitive to the strain and geometry of the π acceptor but less so to polar substituents, and with the exception of sterically hindered alkenes and systems with silicon and phosphorus double bonds, the energy differences between this route and an alternative stepwise process were surprisingly constant. The AM1 method tends to favour a concerted and essentially synchronous transfer of hydrogen whereas MNDO tends to favour a stepwise mechanism, with significant differences also for sterically hindered systems, for the barriers to the concerted hydrogen transfer, and in the disproportionation energies of the intermediate radical pairs involved in the stepwise mechanistic pathway. Highly strained alkene acceptors induce asymmetry in the concerted transfer, and such alkenes also form hydrogen bonded complexes with di-imide. Transition state frontier orbitals are shown to give a simple interpretation of selectivity and reactivity, particularly for strained systems and allene π acceptors. The entropy of activation is suggested to be important in rationalising *cis/trans* alkene selectivity. Bis- α (oxy-anion) substituents on the donor significantly decrease the activation barriers, but induce a stepwise transfer of hydride anion rather than a concerted dihydrogen transfer. Hydrogen kinetic isotope effects show significantly different behaviour for the concerted and stepwise transfer. The concerted [1,4] reduction of butadiene proceeds antarafacially with a much higher barrier than [1,2] reduction. Dimethyl transfer from diazomethane proceeds with double inversion rather than with double retention of configuration at the methyl groups.

The well-known reduction of alkenes by di-imide (1),¹ the hydrogenation of various alkenes and formaldehyde by the iso-electronic species hydroxymethylene (2),² and the transfer of hydrogen from *cis*-4a,8a-dihydronaphthalene (3) to alkenes,³ are all typical examples of a six-electron symmetry-allowed intermolecular dihydrogen transfer reaction. Wide structural diversity is possible in both the π acceptor and the dihydrogen donor, but despite these attractions, relatively few quantitative theoretical studies have been carried out on such systems. The degenerate intermolecular dihydrogen exchange between ethane and ethene was investigated at the SCF and the correlated multi-configuration (MCSCF-FORS) *ab initio* levels,⁴ the coupled hydrogen motion between (2) and ethene was studied at the MP2/6-31G**//3-21G *ab initio* level² and the concerted dihydrogen exchange between methanol and formaldehyde was the subject of two theoretical papers.⁵ There have also been several SCF-MO studies of the reaction between (1) and ethene.⁶ However, no systematic investigation of the effect of substituents and structure on the properties of such reactions has been reported,⁷ and moreover there has been a common assumption that the mechanism for the dihydrogen transfer is concerted and synchronous. Alternative mechanisms, such as those involving stepwise hydrogen-atom transfer, appear not to have been investigated. This may be because the bulk of the experimental evidence accumulated thus far suggests that most of these reactions proceed through a cyclic mechanism. Such evidence includes the observation that the reduction of unsaturated bonds by (1) and (3) occurred in a highly stereoselective manner which suggested that only the *cis* form of the hydrogen donor was involved in the reduction step.^{1,3} Nevertheless, stereospecific *syn* addition could also result from a two-step mechanism where an intermediate radical pair collapses to the products faster than isomerisation by internal rotation. The synchronous mechanistic nature of orbital



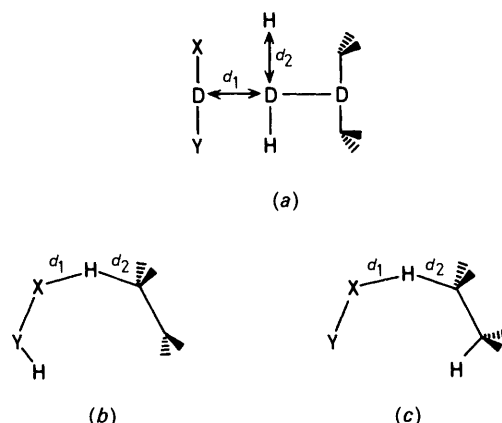


Figure 1. The reaction co-ordinate system used for the construction of the potential energy surfaces of the concerted (*a*) and stepwise (*b,c*) mechanisms of dihydrogen transfer reactions involving (1). D represents a mathematical point (dummy atom) used to facilitate the geometry definition.

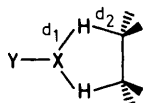


Figure 2. The reaction co-ordinate system used for the construction of the potential energy surface for the concerted mechanism of the reduction of ethene by (4) and formaldehyde.

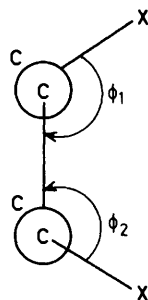


Figure 3. Reaction co-ordinate system used for the construction of the conformational potential energy surfaces for the rotation of the two terminal π bonds in (13) and (12).

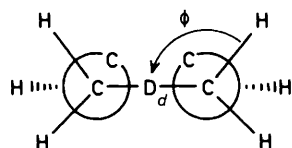


Figure 4. The reaction co-ordinate system used in the construction of the potential energy surface for the electrocyclic ring closure of butadiene.

symmetry-allowed pericyclic reactions such as the Cope rearrangement and the Diels–Alder cycloaddition has been repeatedly challenged by Dewar,⁸ who has proposed on the basis of MNDO and AM1 semiempirical SCF–MO calculations that *e.g.* Diels–Alder reactions normally proceed *via* very unsymmetrical ‘biradicaloid’ transition states. Quite recently, Metzger⁹ reported experimental evidence that supports the thermodynamic feasibility of the symproportionation of alkanes with alkenes involving a radical chain mechanism. Also, it is thought that a radical mechanism is involved in the thermal uncatalysed reduction of aldehydes by alcohols, rather than the alternative synchronous pericyclic dihydrogen transfer.

In the present paper, we report MNDO and AM1 SCF–MO

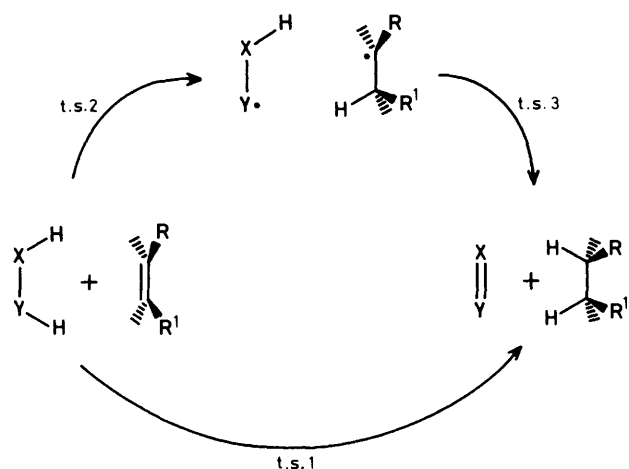
calculations for such reactions for a wide diversity of substrates. The focus was on the balance between a synchronous pericyclic multibond process and an alternative two-step radical pair mechanism, and the effect of a wide range of structural variation in both the dihydrogen donor and the π acceptor on properties such as the barriers to reaction, the structure of the transition state and properties such as kinetic isotope effects.

Computational Procedure.—The calculations were carried out using the MNDO or AM1 SCF–MO procedures¹⁰ employing a standard s/p valence basis set and with full optimisation of all geometric variables. Closed- and open-shell species were investigated at the single determinantal RHF SCF and spin-unrestricted UHF SCF levels, respectively. Where significant spin contamination of doublet states was observed using the UHF method ($\langle S^2 \rangle \gg 0.75$), a variationally exact ‘restricted orbital’ (ROUHF) method which yields pure doublet spin states and exact open shell energies was employed.¹¹ Potential energy surfaces for the concerted dihydrogen transfer reactions were constructed maintaining C_{2v} symmetry for those reactions where this symmetry was present. The energy of the system was calculated as a function of two reaction co-ordinates [Figure 1(*a*)], the projection of the distance of the hydrogens from the migration origin along the C_2 axis (d_1), and the vertical height of the migrating hydrogens (d_2), the remaining geometrical variables being fully optimised. The reaction co-ordinates used for the stepwise route where the distances of the migrating hydrogen from the two termini [d_1 and d_2 , Figures 1(*b*) and 1(*c*)]. The potential surface for the concerted reduction of ethene by (4) was explored varying the N–H and the C–H bond lengths, maintaining C_{2v} symmetry (d_1 and d_2 , Figure 2, X = Y = N). Similar reaction co-ordinates were used for the study of the formaldehyde–ethene system (Figure 2, X = C, Y = O).

The reaction co-ordinates used for studying the conformational surfaces of the *trans* isomers of butenedial (12) and hexa-1,3,5-triene (13) are shown in Figure 3. The conrotatory ring closure of butadiene (C_2 symmetry) and the disrotatory electrocyclic closure of hexa-1,3,5-triene (C_s symmetry) were studied using the length of the C–C developing bond and the dihedral angle of the hydrogen bonded to one of the terminal carbon atoms (d and ϕ , Figure 4). In the contour maps thus produced, approximate saddle points were located and were subsequently refined by minimising the sum of the squared scalar gradients (Bartel’s method). These were characterised by calculating the force constant matrix, which for a genuine transition state, displayed only one negative eigenvalue with the correspondingly correct displacement vectors. In most of the systems studied, the MNDO optimised transition state structures were used as a starting point in the refinement of the AM1 saddle points, and the same technique was followed for systems which differed only in the substituents present. In cases where the transition state geometries predicted by the two methods differed substantially, separate potential surfaces had to be constructed using the AM1 approximation. Thermodynamic properties and kinetic isotope effects were obtained using the rigid rotor, harmonic oscillator model,¹² and the normal vibrational frequencies calculated from the force constant matrix. The molecular orbitals were plotted using a locally modified version of the program psi/77.¹³ Molecular structures and contour maps were plotted using locally developed programs.¹⁴

Results and Discussion

The Reduction of Ethene by the *cis*-Di-imide (1).—We chose to investigate this specific reaction in some depth for several reasons. A minimal number of geometrical variables are involved due to the high symmetry, comparison is possible with



Scheme 1.

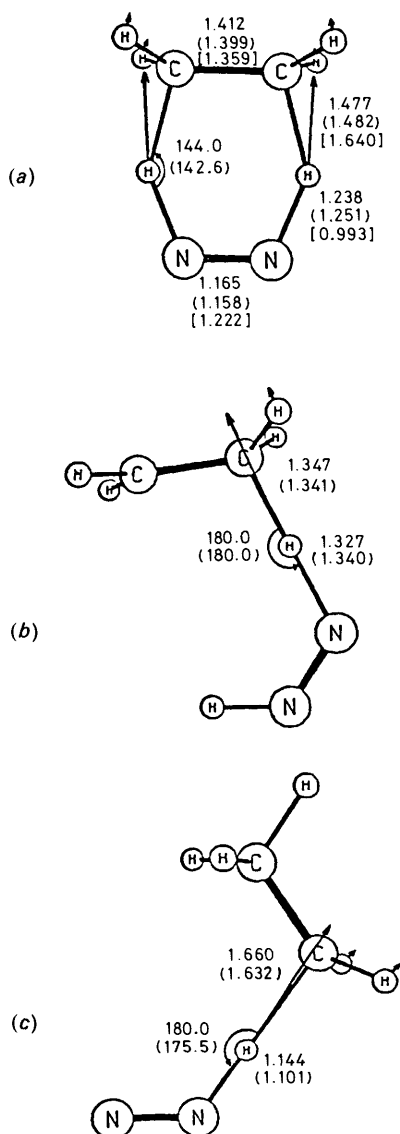


Figure 6. Transition state structures and calculated geometrical parameters for (a) the concerted and (b,c) the stepwise reduction of ethene by (1). Values correspond to MNDO, (AM1) and [STO-3G] calculations.

other theoretical calculations, and much is known about such reactions experimentally. Since only the *cis* form of (1) can act as a stereospecific hydrogenating agent and the reagent as generated *in situ* is almost certainly the more stable *trans*-isomer,¹⁵ the first step in any gas phase reduction must involve an isomerisation to the reactive *cis*-isomer, the mechanism of which¹⁶ seems unlikely to involve simple unimolecular rotation about the N=N bond. The isomeric 1,1-diazene (4) has also been implicated as the dihydrogen transfer agent, although it is significantly higher in energy than (1).

Dihydrogen transfer from (1) is an example of a symmetry allowed $\sigma 4s + \pi 2s$ cycloaddition, with a strong thermodynamic driving force associated with the highly exothermic formation of N₂. Two mechanistic options for this reaction are illustrated in Scheme 1.

Considering first the concerted pathway *via* t.s. 1 (Scheme 1), the calculated MNDO and AM1 potential surfaces indicate that the mechanism is not only concerted but essentially synchronous at the closed-shell RHF level of theory [Figure 5(a)]. Various geometric parameters for the transition state are shown in Figure 6(a).

Where the two semiempirical approximations yield closely related structures, significant differences between these and the previously reported *ab initio* geometries were found. In this context, it must be noted that the latter were obtained at the relatively crude STO-3G level which has been shown to give results that are generally inferior than those for MNDO and AM1.¹⁷ Also, the *ab initio* calculations did not involve dynamical electron correlation, an effect that the semiempirical approximations inherently include through parametrisation. In spite of structural similarities, there is a striking disagreement between the two semiempirical methods regarding the activation energies for the concerted process, which seem to be drastically overestimated by the MNDO procedure. For the hydrogenation of ethene, AM1 gives a barrier (32.3 kcal mol⁻¹) in close agreement with the previous *ab initio* results (26.7 kcal mol⁻¹, 4-31G//STO-3G) reported by Pasto and Chipman.^{6b} The high energy barrier of *ca.* 60 kcal mol⁻¹ reported in another *ab initio* study^{6a} is unreliable, since the putative stationary points were not optimised in full space and were not characterised by inspection of the force constant matrix. It is known that MNDO (and the earlier MINDO/3 treatment) overestimates nuclear repulsions at distances *ca.* 1.5 times the van der Waals distance of the atoms involved, typical of the situation encountered in the transition states of the dihydrogen exchange reactions. The AM1 method differs from MNDO principally by the addition of Gaussian terms describing the core-core repulsions [equation (1)] and considerable improvements over MNDO have been reported,¹⁸

$$\text{CRF}(\text{AB}) = z_A z_B \gamma_{\text{SS}} [1 + F(\text{A}) + F(\text{B})] \quad (1)$$

where

$$F(\text{A}) = \exp(-\alpha_A R_{\text{AB}}) + \sum_i K_{\text{Ai}} \exp[L_{\text{Ai}}(R_{\text{AB}} - M_{\text{Ai}})^2]$$

$$F(\text{B}) = \exp(-\alpha_B R_{\text{AB}}) + \sum_j K_{\text{Bj}} \exp[L_{\text{Bj}}(R_{\text{AB}} - M_{\text{Bj}})^2]$$

in which $F(\text{A})$ and $F(\text{B})$ are atomic functions characteristic of each atom type. In these equations, M_{Ai} is an atomic constant representing the maximum for the Gaussian nuclear repulsion (or attraction) for any given atom. The effect of including equation (1) in the AM1 method can be clearly illustrated for the dihydrogen transfer reactions by evaluating the energy as a function of two reaction co-ordinates and plotting the difference in energy as a contour map¹⁹ (Figure 7).

This clearly reveals that the maximum differences between AM1 and MNDO occur at C-H and N-H distances of about

Table 1. MNDO and AM1 activation energies for the concerted and stepwise pathways for π bond reductions by (1).

π System	1 ^a		2 ^b		3 ^c	
	MNDO	AM1	MNDO	AM1	MNDO	AM1
Ethene	54.7	32.3	43.6	32.8	12.3	0.8
Allene	56.2	34.5	48.2 ^d	39.3	13.2	1.3
			41.3 ^e	31.9	15.4	4.6
Buta-1,2,3-triene	58.8	36.6	41.5	29.7	19.5	7.7
Cyclopropene	50.1	25.0	45.5	26.4	12.3	0.8
Cyclobutene	54.3	27.5	40.3	28.7	13.0	0.5
Cyclobutadiene	47.6	20.5	34.8	19.6	15.7	3.9
<i>trans</i> -Cycloheptene	42.8	17.4	21.9	19.8	16.3	4.8
Methylenecyclopropane	58.2	34.1	44.7 ^f	34.1	14.4	0.5
			46.7 ^g	34.6	12.6	0.8
<i>cis</i> -But-2-ene	61.5	36.2	46.6	35.1	17.6	2.4
<i>trans</i> -But-2-ene	61.3	36.6	46.4	35.5	16.7	2.5
2,3-Dimethylbut-2-ene	72.6	37.1	50.0	33.4	25.2	4.0
Tetracyanoethane	68.0	36.1	45.9	28.7	20.3	6.5
(7; R = Me)	81.7	41.5	63.9	36.5	41.4	13.9
(7; R = Bu ¹)	159.2	99.9				
Benzene	69.9	46.0	46.1	36.4	25.2	6.8
(8)	32.3	7.3	30.2 ^h	15.9	7.3	0.0
			18.8 ⁱ	6.1	14.9	3.0
(9)	38.9	9.3	30.5 ^h	14.2	6.2	0.1
			19.0 ⁱ	6.2	15.2	2.3
(10)	21.5	4.6	16.9	8.8	5.9	0.5
Formaldehyde	66.7	45.5	56.6 ^j	49.4	8.6	3.9
			63.9 ^k	47.6	15.3	4.4
(5)	77.4	64.4	54.3	44.1	20.8	15.2
(6)	66.4	45.1	44.9	31.6		
(16)	36.1		26.1 ^l		13.0	
			35.3 ^m		2.5	
(17)	31.9		25.7		7.3	
(18)	41.4 ⁿ		35.2 ^o		12.8	
			41.7 ^p		2.7	
(19)	24.2 ⁿ		28.2		2.1	
Ethyne	57.6	36.8	48.1	38.3	7.2	0.2
Dicyanoethyne	61.9	36.8	47.7	33.0	13.1	2.3
(11)	65.6 ^q	41.7	53.6	44.2	16.2	5.1
	62.0 ^r	40.0	50.0	39.1		
Benzynes	16.4	0.2 ^s	12.7	1.8	4.0	0.0
Cyclopropane	99.2	73.3	53.6	40.0	13.3	1.1

^a Energy barrier for *t.s.* 1 relative to reactants. All energies in kcal mol⁻¹.

^b Barrier for *t.s.* 2. ^c Barrier for *t.s.* 3 relative to the intermediate radical pair. ^d Via vinyl radical. ^e Via allyl radical. ^f Via tertiary radical. ^g Via primary radical. ^h Via the tertiary bicyclic radical. ⁱ Via the secondary bicyclic radical. ^j Via hydroxymethyl radical. ^k Via methoxy radical. ^l Via silylmethyl radical. ^m Via methylsilyl radical. ⁿ Phosphorus parameters are not available for AM1. ^o Via phosphylmethyl radical. ^p Via methylphosphyl radical. ^q Reduction of the non-conjugated p system. ^r Reduction of the conjugated p system. ^s The displacement vector associated with the imaginary frequency characterising the transition state did not correspond to a concerted transfer of two hydrogen atoms to benzyne.

1.7 Å, almost exactly coincident with the transition state values. These results strongly support the argument that the discrepancies between MNDO and the *ab initio* results may often be related to the over-simple form of the core repulsion function used in the MNDO. We do note however that in our previous study of dipolar cycloaddition,¹⁹ cheletropic,²⁰ and sigmatropic reactions,¹⁹ the published¹⁸ parameter M_A for one of the Gaussian terms for nitrogen (2.1 Å) was suspected to be incorrect. A simple modification¹⁹ to the nitrogen parameter (1.6 Å) converted an asynchronous AM1 potential surface for the reaction between HN₃ and ethyne into a synchronous one. A contrasting result was obtained for cheletropic elimination of nitrogen,²⁰ where the potential remained asymmetric. When such a modification was applied to the ethene/(1) system, a

further 6.5 kcal mol⁻¹ reduction in the activation barrier to 25.8 kcal mol⁻¹ was obtained; a value that compares more favourably with the 4-31G calculation.^{6b} However, unlike the example of dipolar cycloaddition reactions, this modification induced no qualitative change in the potential energy surface for the reaction. This lowering in energy is likely to be less for more asymmetrical dihydrogen transfers.

We consider next the stepwise route *via t.s.* 2 and *t.s.* 3 [Figure 5(b),(c), and 6(b)(c)]. The rate-determining step for the stepwise process is unambiguously the formation of the radical pair (*t.s.* 2, Table 1), although the activation energies for the disproportionation of these radicals to products (*t.s.* 3) is also of interest (*vide infra*). At the MNDO level, the energy of *t.s.* 2 is 11.1 kcal mol⁻¹ lower than that for the synchronous route (*t.s.* 1), whereas the AM1 method (using the published parameters) indicates the stepwise and synchronous pathways to be virtually identical in energy (Table 1). However, if the alternative value (1.6 Å) of the nitrogen core repulsion function is used, the AM1 barrier for *t.s.* 2 is reduced by only 2.0 kcal mol⁻¹ which is 4.5 kcal mol⁻¹ less than for the concerted reaction. Further factors which favour the latter mechanism are that the energies of the biradical-like transition states are likely to be underestimated by the UHF method employed, due in part to triplet state contamination of the wavefunction (*vide infra*), and the probability that electron correlation corrections will significantly reduce the energy of *t.s.* 1.² These various factors lead to the overall conclusion that AM1 distinctly favours the synchronous pathways (*t.s.* 1), while MNDO more distinctly predicts the stepwise pathway (*t.s.* 2) as the lowest energy route.

The two semiempirical approximations were in a striking disagreement regarding the value of the barrier to *t.s.* 3 measured relative to the radical pair. Such a radical disproportionation seems likely to require a small enthalpic barrier,²¹ and indeed the AM1 value is only 0.8 kcal mol⁻¹. The MNDO barrier of 12.3 kcal mol⁻¹ appears qualitatively incorrect (Table 1). The energies of the intermediate radical pair were also calculated using a variationally exact open-shell restricted Hartree-Fock (ROUHF) procedure, the results being only 1.9 (MNDO) or 2.0 kcal mol⁻¹ (AM1) above the UHF results. It is reasonable to assume that the errors introduced by use of the more approximate UHF formalism for calculating this barrier are of a similar order, since *t.s.* 3 is a very early transition state. Indeed the finite barrier of 0.8 kcal mol⁻¹ obtained at the AM1 level for *t.s.* 3 may be entirely due to such an error. It is also clear that use of the UHF approximation does not explain the much larger MNDO barrier, which is more probably due to the inadequacies of the core repulsion function. The joint energy of the intermediate radical pair was predicted to be 6.3 (MNDO) or 8.2 (AM1) kcal mol⁻¹ above the reactants at the UHF level, which leads to a significant reverse barrier (recombination of the intermediate radical pair back to the reactants) at both the semiempirical levels (37.3/MNDO, 24.6/AM1). Although *t.s.* 1 does not closely resemble the radical pair, and therefore no quantitative estimate of the UHF error can be made, the magnitude of this barrier suggests that it may be real.

The Reduction of Ethene by (4).—It has been previously suggested¹⁶ that *syn* hydrogenation of alkenes by N₂H₂ may proceed *via* species (4) rather than (1). Such a reaction also corresponds to a six-electron process and indeed the calculated potential surface (Figure 8) shows it to be a concerted allowed reaction with a synchronous structure (Figure 9) at the RHF level. The calculated (AM1) barrier from (4) (30.0 kcal mol⁻¹) is slightly less than that found for (1). The stepwise pathway (22.0 kcal mol⁻¹) is noticeably more stable than the analogous route *via* (1). Despite this, (4) is calculated to be 23.3 kcal mol⁻¹ higher in energy than (1), and the overall conclusion must be that reductions do not normally proceed *via* 1,1-diazenes.

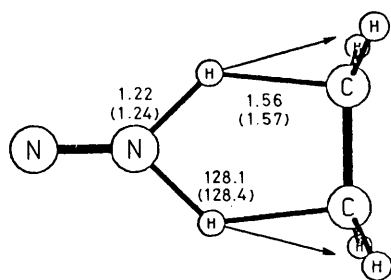


Figure 9. MNDO (AM1) calculated transition state structure for the concerted reduction of ethene by (4).

The Reduction of Substituted π -Bond Systems by (1).—Enormous structural diversity is possible in the dihydrogen acceptor, and this is reflected in the unusually large span of values for ΔH^\ddagger for the concerted process (Table 1). The magnitude of the barrier is closely related to the geometry and stability of the reactant alkene or alkyne, and the product dihydro derivative. Interestingly, the energy difference between the concerted pericyclic and two-step radical pair mechanisms is largely (with some exceptions discussed below) unaffected by structural variations in the dihydrogen acceptor, or by the enthalpic barrier for the reaction. While AM1 consistently predicts a fine balance between the two mechanisms, the MNDO figures indicate a much clearer preference for the open shell route. This balance appears to be affected by polar substituents such as cyano, which stabilise the radical centre formed in the stepwise route, but slightly destabilise the concerted pathway (*cf.* tetracyanoethene, Table 1). Also noteworthy is that the transition states for the reduction of asymmetric double bonds retain a significant degree of synchronicity in the hydrogen transfer. For example, that for the reduction of methylenecyclopropane is quite symmetric (1.49/1.49 Å for the two forming C-H bonds and 1.24/1.24 for the two N-H bonds) despite the differing degrees of strain on the two carbon atoms of the reactant.

Compared with the parent system, several conjugated or hindered alkenes show larger calculated AM1 barriers for the radical disproportionations *via t.s. 3* (Scheme 1). For example, the stepwise reduction of allene can form either a vinyl radical or an allyl radical, the latter showing a significantly lower barrier for *t.s. 2*, as expected based on product stability, but a higher barrier for *t.s. 3* (Table 1). The origins of the increased and probably erroneous barrier to *t.s. 3* can be traced to greater spin contamination in the UHF wavefunction for delocalised radicals such as allyl compared with the localised vinyl radical. Whereas the difference in the UHF and the variationally exact ROUHF procedures for localised radicals is ≤ 2.5 kcal mol⁻¹, the value calculated for allyl radical is 7.6 kcal mol⁻¹. Similarly significant disproportionation barriers calculated for butatriene, cyclobutadiene, and benzene are all probably due to this error. There are two further classes of reaction where the barrier to *t.s. 3* is significantly non-zero. One of these (5) is discussed below. The other is observed for sterically hindered systems, such as (7; R = Me) and to a lesser extent tetramethylethene. In these cases, there is every reason to believe that these barriers are indeed genuine.

Dihydrogen Transfer to N=N π -Bond Systems.—Merz and Reynolds have recently reported²² an AM1 study of tautomerism in free-base porphyrins, from which they conclude that hydrogen migration occurs *via* a mechanism involving two sequential [1,5] hydrogen shifts between adjacent nitrogen atoms, rather than a synchronous dihydrogen shift. The latter, which correspond to a second-order saddle point, was

calculated to be 26.2 kcal mol⁻¹ higher in energy. Our AM1 results for dihydrogen transfer between carbon and nitrogen indicate that the barrier for dihydrogen relative to single hydrogen transfer may be reduced by 4.5 kcal mol⁻¹ by modification of the core repulsion function. This suggests that the barriers for transfer exclusively between nitrogen atoms may be reduced even further with such a modification. To investigate this further, we studied two such systems, (5) and (6). The latter is an unusually good diene trap indicating a particularly reactive N=N double bond. The AM1 barrier for the concerted reduction of (5) was unusually high (64.4), and this result was also unique in that the difference between the concerted and stepwise pathways was almost the same at the MNDO and AM1 levels (Table 1). Changing the core repulsion function in the manner described above reduced the value of the concerted barrier for dihydrogen transfer by as much as 19.0 kcal mol⁻¹. This result may have considerable bearing on the porphyrin proton-transfer kinetics discussed by Merz and Reynolds.²³ The AM1 results for (6) are even more anomalous. We had hitherto always succeeded in characterising stationary points for concerted dihydrogen transfers as genuine transition states, at the MNDO as well as the AM1 levels. However, the AM1 results for concerted transfer to (6) gave a symmetrical stationary point with *two* negative force constants, the smaller corresponding to an asymmetrical distortion. Such behaviour had been previously noted for C-N bond forming reactions at the AM1 level.^{19,20} Employing the revised core repulsion function did not induce qualitative changes in the potential surface, but resulted in a reduction of the second negative root of the AM1 Hessian by 237i cm⁻¹. Although the calculated activation energy (34.1 kcal mol⁻¹) was still greater than for ethene itself, the second imaginary frequency was still high (555i cm⁻¹), suggesting that a proper reoptimisation of the AM1 nitrogen parameters is likely to reduce this barrier even further. We do note, however, that the reactivity of (6) as a diene trap might in part be due to the type of secondary orbital interactions not possible in the di-imide reaction.

The Reduction of Sterically Hindered π -Bond Systems by (1).—Several entries in Table 1 reveal a striking disagreement between MNDO and AM1 in the predicted enthalpic barriers for sterically hindered systems. The substitution of the four hydrogen atoms of ethene by methyl groups corresponds to a steric effect of 17.9 and 6.4 kcal mol⁻¹ for the concerted and the stepwise path with MNDO, but of only 4.8 and 0.6 kcal mol⁻¹ respectively with AM1. For (7; R = Me), the steric effects for the two mechanisms are 27.0/20.3 (MNDO) and 9.2/3.7 (AM1), respectively, and for the most hindered system (7; R = Bu') the steric effect for the concerted path of 104.5 (MNDO) or 67.6 (AM1). These differences between AM1 and MNDO reflect one of the well-known major weaknesses^{10a} of the latter, *i.e.* the tendency to overestimate energies for crowded molecules, also attributed to the erroneous treatment of the non-bonded interactions. This observation that the stepwise pathway is subject to a smaller steric effect suggests that as steric hindrance increases, there could be a switch from an exclusively synchronous mechanism to one involving the formation of an intermediate radical pair. Since the barrier to *t.s. 3* also increases (see above), the reaction may also cease to be stereospecific as the lifetime of the intermediate radicals increases.

Another geometrical aspect is the experimentally observed selectivity of (1) for *trans* rather than for *cis* double bonds.^{1c} MNDO does indeed show a small preference in this sense, whereas AM1 appears to slightly favour *cis* hydrogenation (Table 1). At the transition state, any pair of *cis* substituents will approach each other more closely due to the change from sp² to sp³ hybridisation at the carbon centres. The tendency of MNDO to overestimate such non-bonded interactions may

Table 2. MNDO and AM1 activation energies for the concerted and stepwise pathways for dihydrogen transfer reactions.

Donor	π System	1 ^a		2 ^b		3 ^c	
		MNDO	AM1	MNDO	AM1	MNDO	AM1
Ethane	Ethene	81.2	52.4	49.7	39.0	24.4	7.4
Ethane	Allene	82.3	53.7	50.5 ^d	40.3	22.2	5.2
				44.2 ^e	33.7	29.9	13.1
Ethane	Ethyne	82.2	57.0	54.5	44.6	16.2	3.0
(20)	Ethene	78.1	52.1	44.7	35.0	26.8	10.1
(22)	Ethene	76.5	51.2	44.6	34.6	25.3	10.7
(21)	Ethene	46.6	21.5	23.1	10.1	6.8	0.0
(23)	Ethene	48.0	21.4	9.3	10.4	84.4	61.3
(23) ^l	Ethene	66.4	33.7	23.0	12.7	10.2	3.2
(23) ^m	Ethene	71.6	44.1	33.0	22.0	17.8	6.6
1,2-Difluoroethane	Ethene	78.7	51.5	45.2	34.4	25.2	8.7
Cyclohexa-1,3-diene	Ethene	71.0	41.0	42.5	30.4	22.4	6.2
Cyclohexa-1,3-diene	Allene	72.8	42.7	42.6 ^d	30.9	22.4	4.1
				39.7 ^e	29.5	27.5	11.0
2,3-Dihydronaphalene	Ethene	68.5	38.1	41.1	27.9	22.6	6.4
(3)	Ethene	62.9	32.4	38.0	25.0	19.0	3.7
Cyclobutene	Ethene	96.9	71.6	48.0	39.4	29.8	14.7
Hydrogen peroxide	Ethene	104.6	57.5	59.8	42.2	35.9	10.5
Hydrogen peroxide	Allene	104.3	60.2	65.2 ^d	42.7	32.2	7.1
				62.0 ^e	38.7	47.5	33.1
Methanol	Formaldehyde	87.2	52.5	55.2 ^f	57.1	15.2	2.4
				66.5 ^g	53.8	3.8	5.7
		96.1	62.7	99.9 ^h	76.3	21.4	4.4
				62.5 ⁱ	51.0	30.6	6.4
(19)	Ethene	39.8		28.8		8.7	
(2)	Ethene	53.7	19.4	40.4 ^j	22.2	17.4	3.1
				37.6 ^k	28.6	21.2	2.5
(4)	Ethene	48.5	30.0	32.3	22.9	13.5	0.8
(4)	(10)	23.7	10.9				
(1)	Butadiene ⁿ	98.1	70.3	36.8	26.1	15.7	4.6
(1)	(24)	84.8	60.1				
(25)	Ethene	170.8 ^o	153.6	125.1	104.6	69.0	53.8
		158.6 ^p	126.3	75.8	70.5	42.4	17.5
Formaldehyde	Ethene	70.7	44.4	45.9	34.8	17.4	3.1

^a Energy barrier for *t.s.* 1 relative to reactants. All energies in kcal mol⁻¹. ^b Barrier for *t.s.* 2. ^c Barrier for *t.s.* 3 relative to the intermediate radical pair.

^d Via vinyl radical. ^e Via allyl radical. ^f O to O hydrogen atom migration in the first step. ^g C to C hydrogen atom migration in the first step. ^h O to C hydrogen atom migration in the first step. ⁱ C to O hydrogen atom migration in the first step. ^j O to C hydrogen atom migration in the first step. ^k C to C hydrogen atom migration in the first step. ^l Results for a unipositive hard-sphere with ionic radius 0.7 Å with position optimised with respect to the oxygen atoms. ^m Results for a dipositive hard-sphere with ionic radius 0.7 Å. ⁿ Energies correspond to 1,4 transfer of dihydrogen to the diene. ^o Methyl migration with retention of configuration at the migrating centre. ^p Methyl migration with inversion of configuration at the migrating centre.

Table 3. MNDO and AM1 activation energies (in kcal mol⁻¹) for the electrocycloisomerisation reactions.

	MNDO	AM1
Butadiene	51.4	50.4
(14)	48.0	49.1
Hexa-1,3,5-triene	38.5	29.5
(15)	32.9	21.5

explain the preference of this particular method for *trans* reaction. The AM1 method is less prone to such errors and so alternative explanations for the *trans* selectivity must be sought. One such explanation, in terms of the entropic contributions, is discussed below.

Complex Formation between Highly Strained Systems and (1).—In a previous MNDO study of benzyne, we noted²³ that this species is predicted to have a significant dipole moment, the negative end of the dipole being exocyclic to the ring. Since (1) also has a significant dipole moment, the possibility arises of an interaction between this species and both benzyne and strained systems such as compounds (8)–(10). For all the systems, the

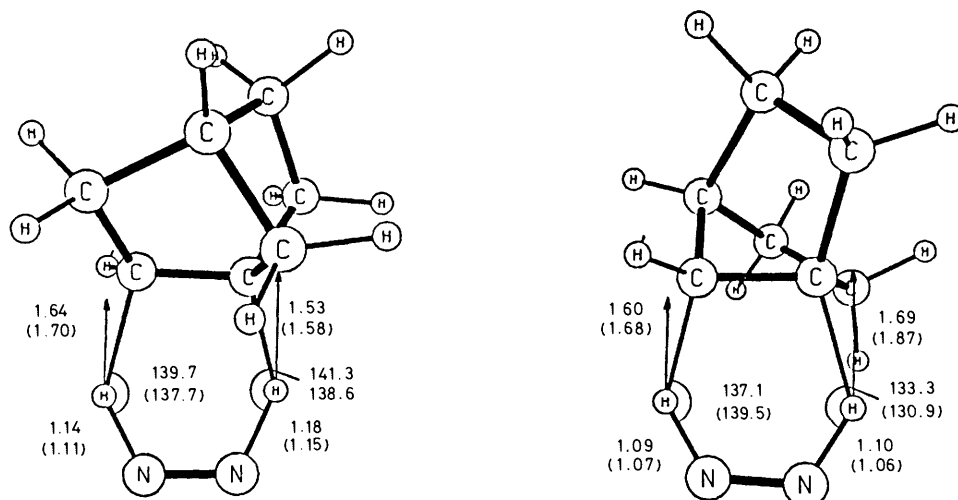
optimised supermolecule indeed had an energy significantly lower than the sum of the individual systems (Table 4). These systems represent almost unique examples of the formation of a significant hydrogen bond to an alkene acting as an acceptor rather than a hydrogen donor.

The Reduction of Strained π -Bond Systems of (1).—When the reduction of the π bond results in release of strain in the dihydrogen acceptor, the barriers to reaction appear significantly decreased. This is evident from the activation energies for the reduction of cyclopropene, cyclobutene, *trans*-cycloheptene and the fused cyclic systems (8)–(10), which are lower than that for ethene itself. The order of hydrogenation of these substrates is roughly consistent with the relative strain imposed on their π bonds, but some subtle differences regarding twisted double bonds cannot be explained by this means. If the spatial orientation of the π -type HOMO of the alkene is such as to facilitate overlap with the σ N–H type LUMO of the (1), the energetic demands of the reaction decrease substantially. For example, the activation energies are extremely low for alkenes containing double bonds where the two p-orbitals remain coplanar but are 'folded back,' such as benzyne and (10).²⁴ We should point out, however, that we were unable to locate a genuine transition state for the concerted reduction of benzyne at the AM1 level.

Table 4. MNDO and AM1 heats of formation (in kcal mol⁻¹) for dipole stabilised complexes.

Donor (A)	π System (B)	(A + B) ^a		[AB] ^b		(A + B) - [AB]	
		MNDO	AM1	MNDO	AM1	MNDO	AM1
(1)	Benzyne	172.8	172.9	172.3	168.8	0.5	4.1
Water	Benzyne	77.7	81.2	77.3	80.0	0.4	1.2
Hydrogen peroxide	Benzyne	107.2	112.2	106.7	109.2	0.5	3.0
(1)	(9)	110.3	112.2	109.8	108.5	0.5	3.7
(1)	(9)	133.2	138.5	132.6	134.3	0.6	4.2
(1)	(10)	148.3	160.0	147.6	155.3	0.7	4.7

^a Sum of the calculated heats of formation of the isolated molecules. ^b Calculated heat of formation of the supermolecule (optimised intermolecular distance).

**Figure 10.** MNDO (AM1) calculated transition state structures for the concerted reduction of (a) (8) and (b) (9) by (1).

The eigenvector associated with the imaginary frequency characterising the saddle point in the potential surface, did not correspond to the concerted transfer of two hydrogen atoms to benzyne, probably due to the employment of numerical rather than analytical derivatives in the evaluation of the Hessian matrix. An unusual effect is observed for species containing twisted π bonds, such as the two bicyclic alkenes (8) and (9). The latter is less stable than (8) by 22.9 (MNDO) or 26.3 (AM1) kcal mol⁻¹, and so might be expected to be significantly more reactive. Instead, the AM1 barrier for concerted hydrogen exchange is actually higher by 2.0 kcal mol⁻¹, due entirely to the significant degree of non-planarity in the transition state (Figure 10).

The frontier orbitals for this reaction (Figure 11) show how the reduced overlap as a result of the greater degree of twisting in the double bond results in raising the energy of the ideally planar activated complex. The two forming C-H bonds for this hydrogenation are 1.60 and 1.69 Å (MNDO) or 1.68 and 1.87 Å (AM1), corresponding to the least synchronous concerted transition state of all the systems studied. The discrimination between (8) and (9) is not evident in the stepwise mechanism, where the first hydrogen is delivered to either C² or C⁷ to form a common intermediate, and where the angle between the two p-orbitals of the double bond is not important in determining the energy of the transition state. In almost all the other cases, the stationary points are symmetrical and correspond to essentially synchronous processes. The preceding arguments rely to a certain extent on the geometrical characteristics of the cyclic six-membered ring transition state. Since reduction by the species (4)

proceeds *via* a five-membered ring transition state with different geometrical requirements, it was also of interest to study the hydrogenation of the severely strained alkene (10) by this donor. Whereas ethene is reduced more easily by (4) than by (1), as expected from a more exothermic reaction, this order is actually inverted in the case of (10) (Table 2). This can be attributed to the decreased overlap of the relatively more 'compact' HOMO of (4) with the highly bent π -type LUMO of the alkene. These results suggest that the relative reactivities of (1) and (4) are not a consequence of an intrinsic difference in their hydrogen donating capability, but rather are dominated by the effectiveness of the frontier orbital overlap.

The Reduction of Butynedial (11) by (1).—This alkyne possesses two orthogonal central π bonds, only one of which is strongly conjugated with the two carbonyl groups. There could in principle be two transition states corresponding to synchronous reduction of (11) by (1), involving attack on either the orthogonal or the conjugated double bond, the former giving a conjugated product (12) and the latter a system where the two carbonyl groups are both orthogonal to the alkene π bond. MNDO is known¹⁰ to incorrectly predict the two carbonyl groups in glyoxal to be orthogonal, and for this reason we wished to calibrate the MNDO and AM1 conformational surfaces of the *trans*-isomer of (12) and also that of hexa-1,3,5-triene, (13) [Figures 12(a) and (b)]. The *trans*-isomers were selected for this study because close internuclear separations for certain values of the two rotational reaction co-ordinates led to computational difficulties for the *cis*-isomers.

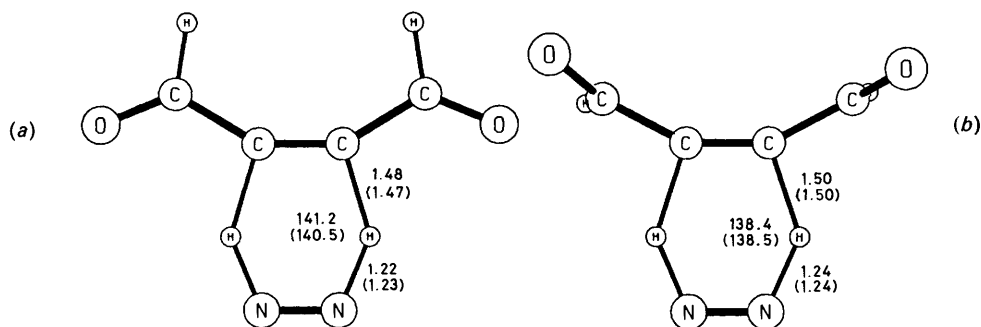
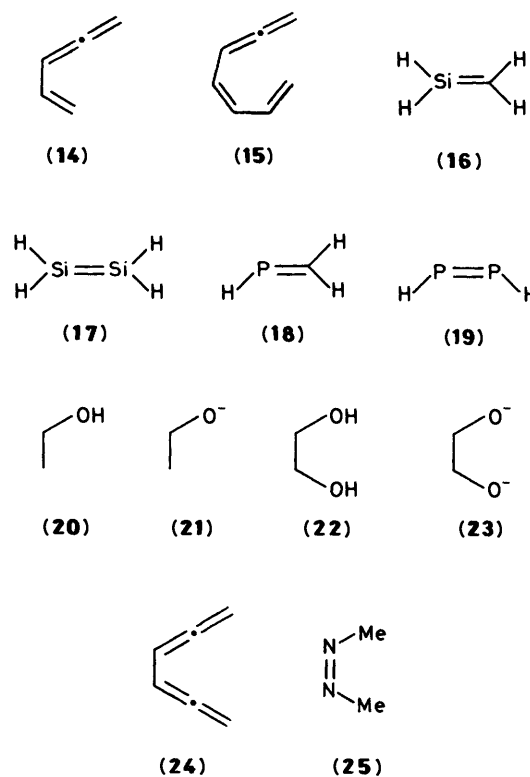


Figure 13. MNDO (AM1) calculated transition state structures for the concerted reduction of (a) the conjugated and (b) the orthogonal π bonds of (11) by (1).

The potentials are qualitatively quite different, showing that only AM1 predicts the stable form of *trans*-(12) to be planar and conjugated, thus confirming that the MNDO is qualitatively unable to reproduce the conformational properties of such systems. The AM1 method predicts that the conjugated isomer of *cis*-(12) is more stable by 11.6 kcal mol⁻¹ (and indeed by 6.7 using MNDO) than the orthogonal form ($\phi_1 = \phi_2 = 90^\circ$ on the contour diagram).

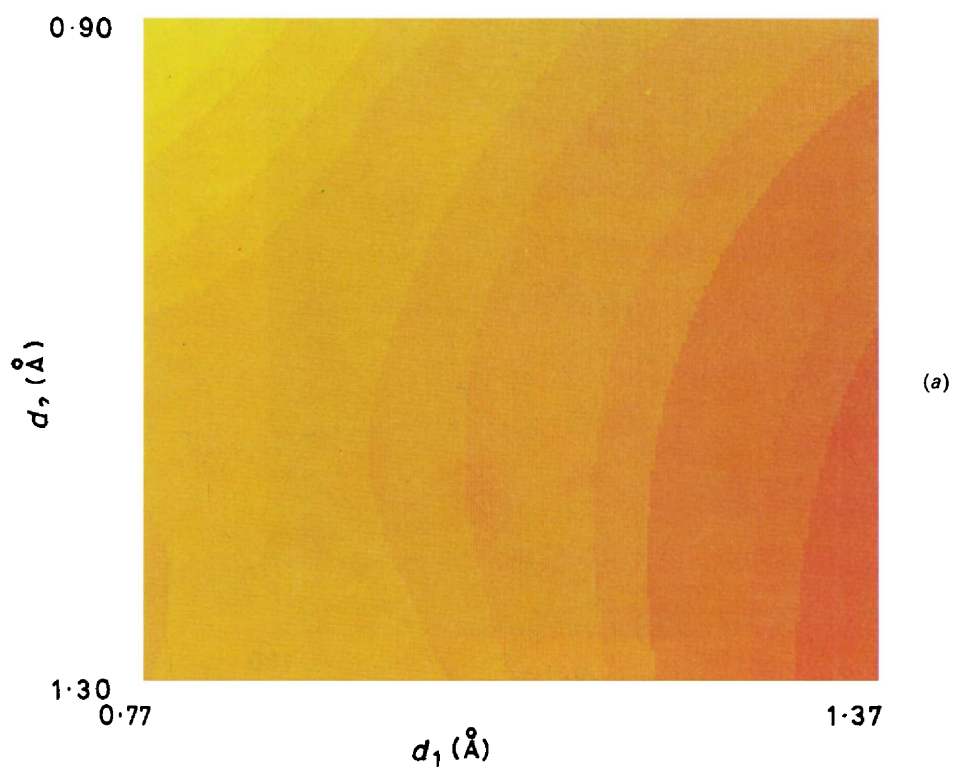
These conclusions suggest therefore that a product-like transition state would lead to reduction of the orthogonal π bond in (11) in preference to the conjugated one. Two genuine transition states were located (Figure 13) of which reduction of the conjugated π bond was energetically favoured over the orthogonal π bond by 3.6 (MNDO) and 1.7 kcal mol⁻¹ (AM1, Table 1), contrary to the arguments above. The origins of this effect can be traced to the nature of the frontier orbital (HOMO/LUMO) interactions associated with the magnitude of the energy difference between the two levels and the extent to which these orbitals are allowed to overlap. Thus, the delocalised π -type LUMO of the alkyne (-0.82 eV/AM1) lies lower than the orthogonal system (0.65 eV/AM1) in the MO manifold, and therefore interacts better with the low lying σ -type HOMO of (1) (-10.57 eV/AM1). Moreover, the electron density in the conjugated π -type orbital is diffused away from the central carbon-carbon bond through conjugation, adopting a more favourable orientation towards the interacting σ -type HOMO of (1). This in turn results in a lowering of the activation energy for the process to an extent sufficient to overcome the thermodynamic handicap. A similar argument was used above to account for the differences in reactivity of (8) and (9), and was also used to analyse subtle effects in the cycloaddition reactions between S_4N_4 and dicyanoethyne.²⁵

The Reduction of Cumulenes by (1).—It has been previously experimentally observed that the double bonds in cumulenes such as allenes are more reactive towards thermal electrocycloaddition or cycloaddition than the homologous alkene.²⁶ However, the reactivity of such allenes towards a dihydrogen transfer agent such as di-imide is unknown. We wished initially to confirm this pattern of reactivity theoretically, choosing as model systems the electrocyclic ring closures of butadiene, hexatriene and the two corresponding allenes (14) and (15) (Table 3). The potential surface for the reaction of butadiene is shown in Figure 14, together with the calculated transition state structures (Figure 15). The calculated barriers to ring closure for butadiene were 51.4 (MNDO) and 50.4 (AM1) while those for (14) were 48.0 and 49.1 kcal mol⁻¹, respectively. The allene (14) is seen to be only slightly more reactive than butadiene. However, few butadienes cyclise thermally to cyclobutenes (the reverse reaction being the more common), and the experimental observations referred to above relate to

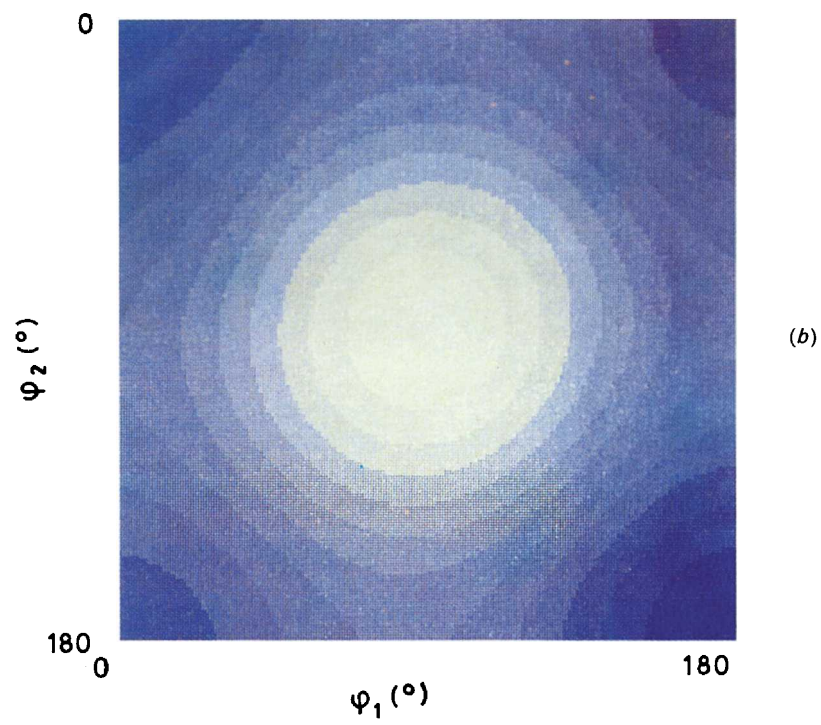
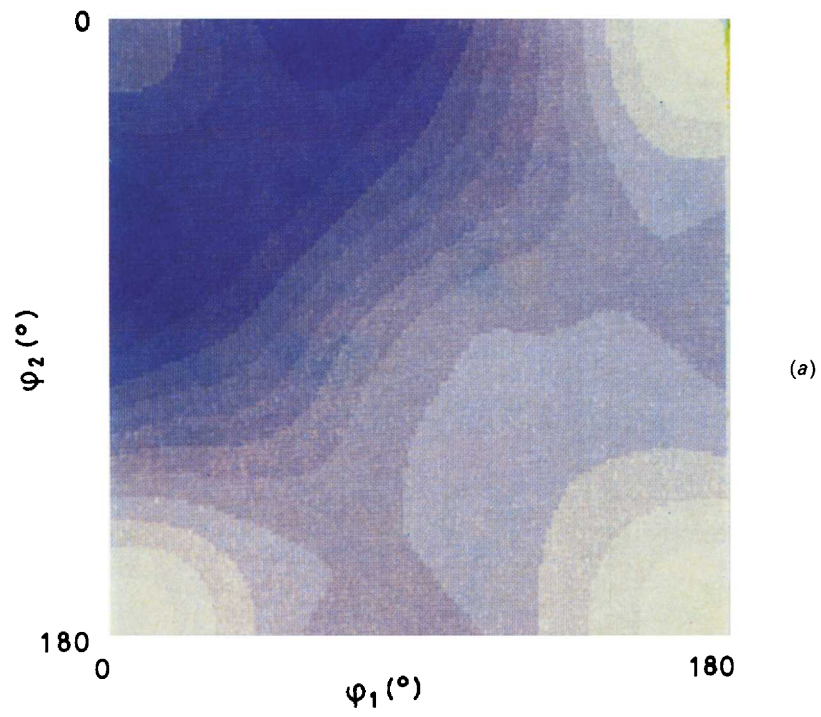


the cyclisation of hexatrienes. The analogous calculated barriers for hexa-1,3,5-triene *versus* (15) were 38.47/32.90 (MNDO) and 29.49/21.45 kcal mol⁻¹ (AM1). This now corresponds to a clear effect, with a lower barrier for the cummulene of 8.0 kcal mol⁻¹. This is in reasonable accord with the experimentally manifested reactivity of allene.²⁶ Inspection of the frontier orbitals provides a simple explanation of this phenomenon (Figure 16). That for butadiene corresponds to formation of a σ bond, the original conjugated π system being largely disrupted. In contrast, the allene homologue involves major participation from the originally orthogonal π -system, with greater retention of π conjugation in the HOMO. This effect is increased for the hexatriene/(15) system due to more favourable geometrical features and an emerging delocalised system.

Having established that both MNDO and AM1 correctly reproduce the effect of an allene in pericyclic C-C bond formation, we considered next dihydrogen transfer to an allene. Here the barrier to di-imide reduction was found to be 2.2 kcal mol⁻¹ higher than for ethene, and the next cumulene (buta-1,2,3-triene) was even less reactive by 4.3 kcal mol⁻¹ (Table 1). The



To face page 482]



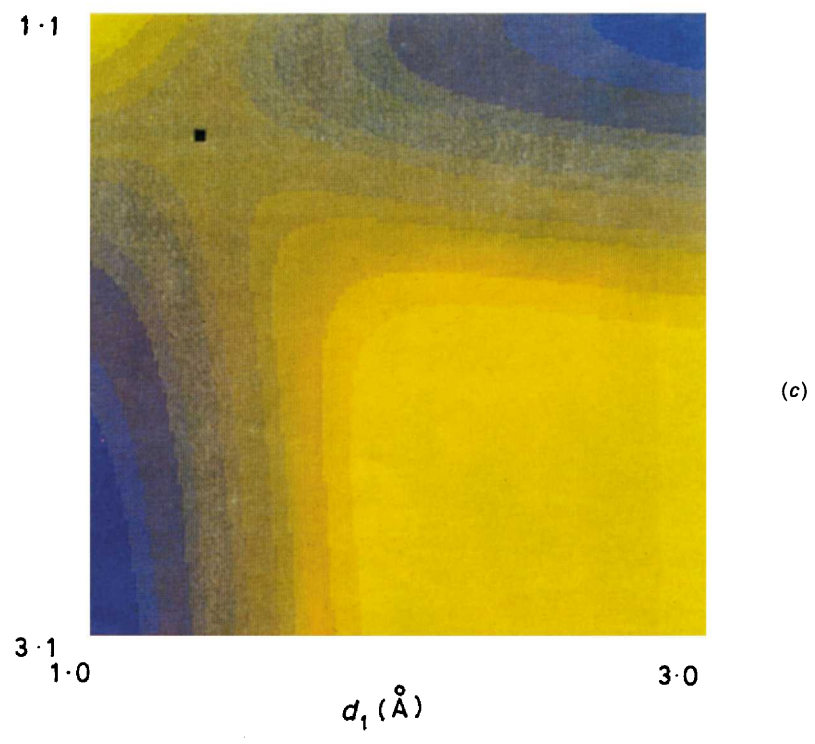
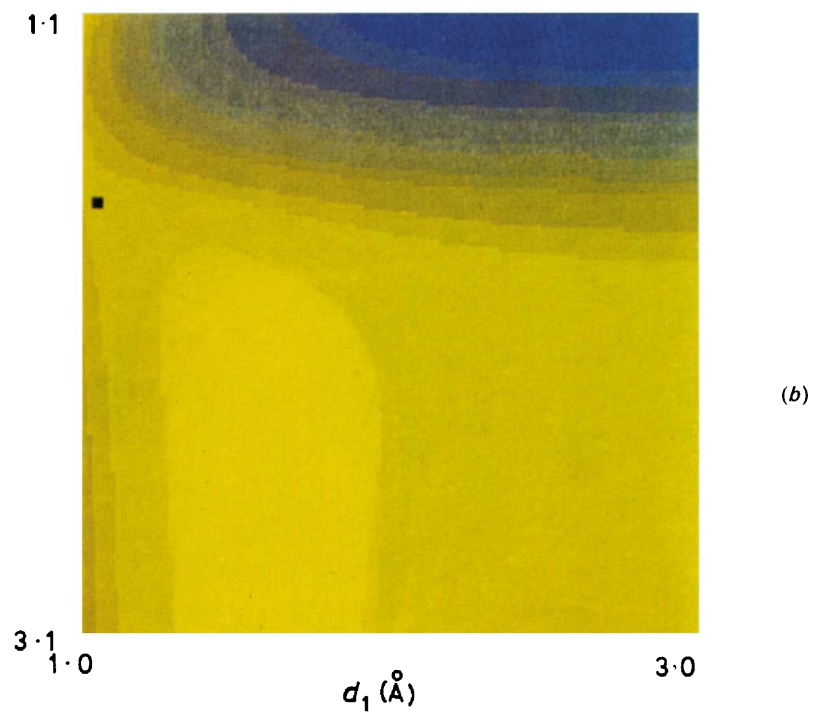


Figure 5. MNDO potential energy contour maps for the concerted (a) and stepwise (b), (c) reduction of ethene by (1).

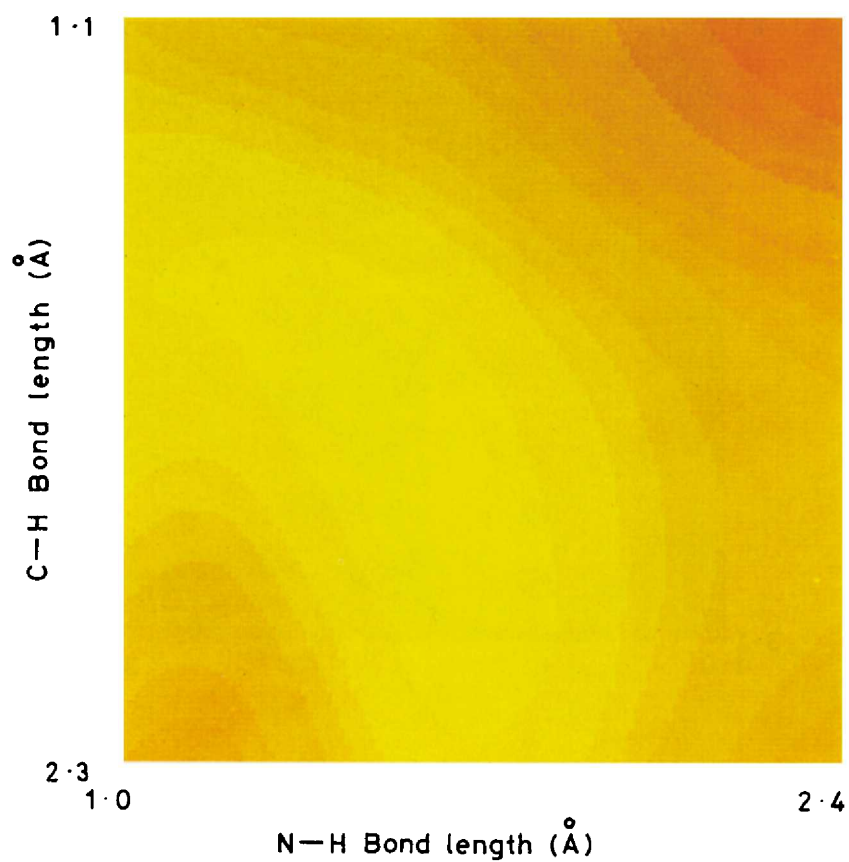


Figure 7. Contour map of the energy differences between the MNDO and AM1 potential surfaces for the concerted reduction of ethene by (1).

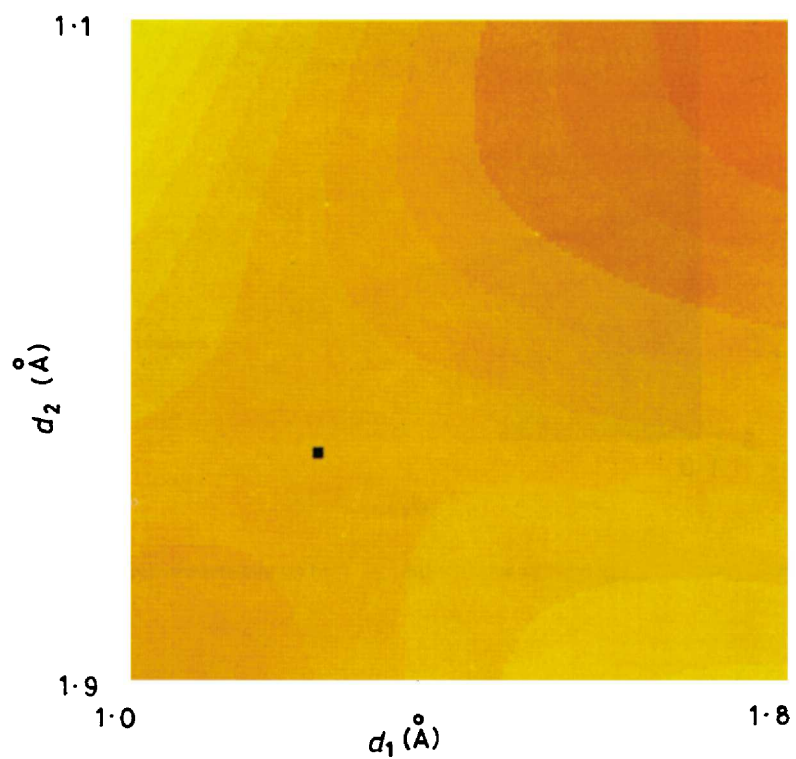


Figure 8. AM1 potential energy contour map for the concerted reduction of ethene by (4).

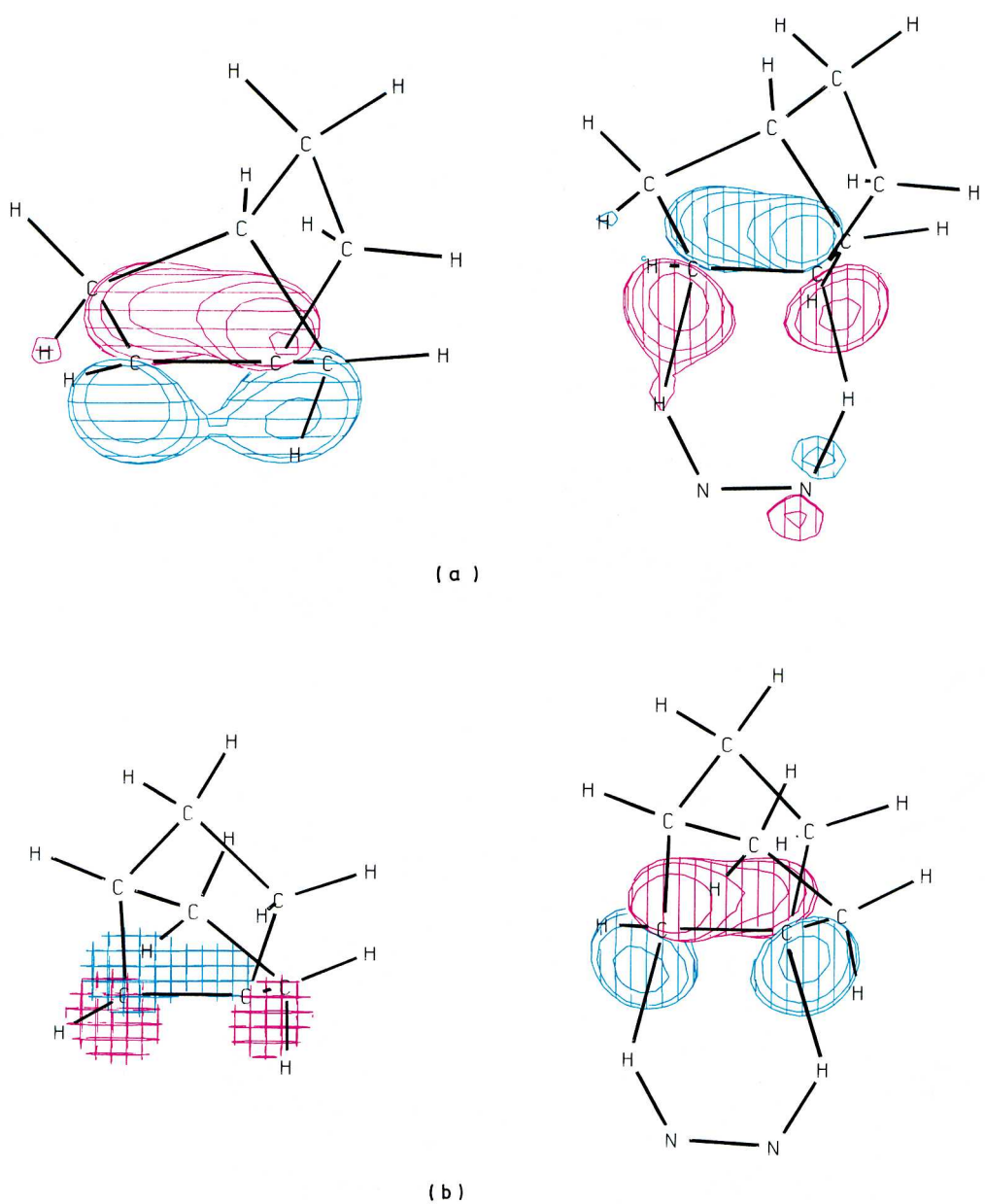


Figure 11. The AM1 π type alkene HOMO and its interaction with the σ N-H type LUMO of di-imide for (a) (8) and (b) (9).

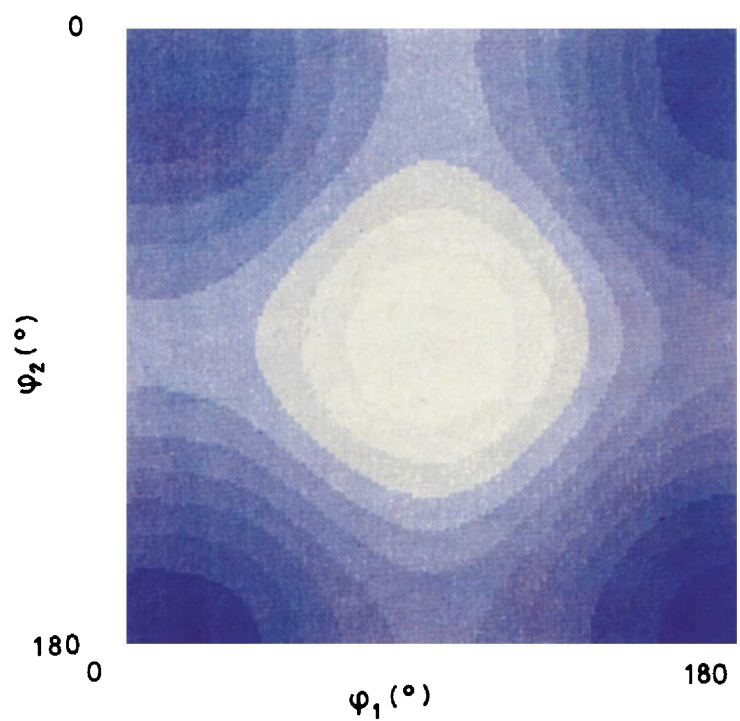
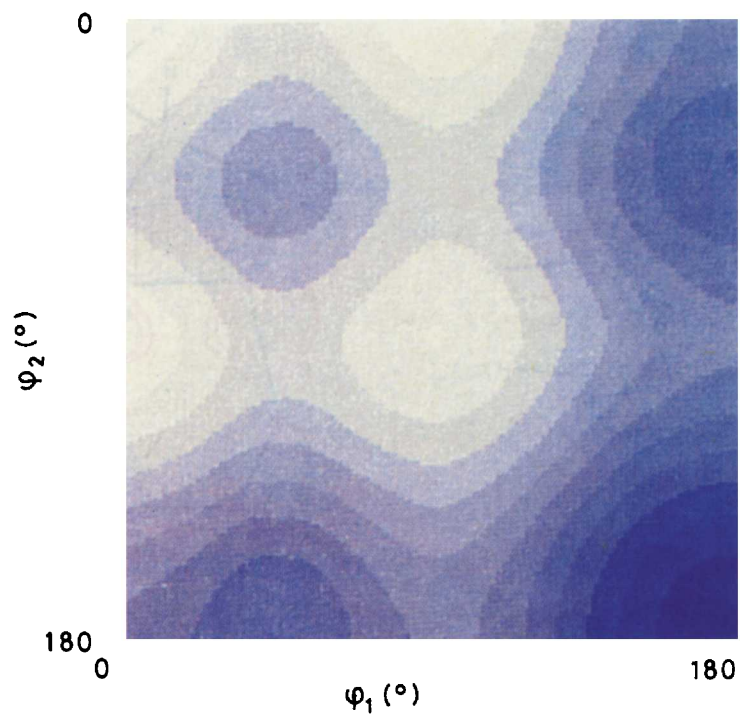


Figure 12 MNDO (a) and AM1 (b) conformational potential energy contour maps for the rotation of the two terminal π bonds in *trans*-(13), and (c) and (d) the rotation of the two carbonyl groups in *trans*-(12). Reaction co-ordinates are defined in Figure 3.

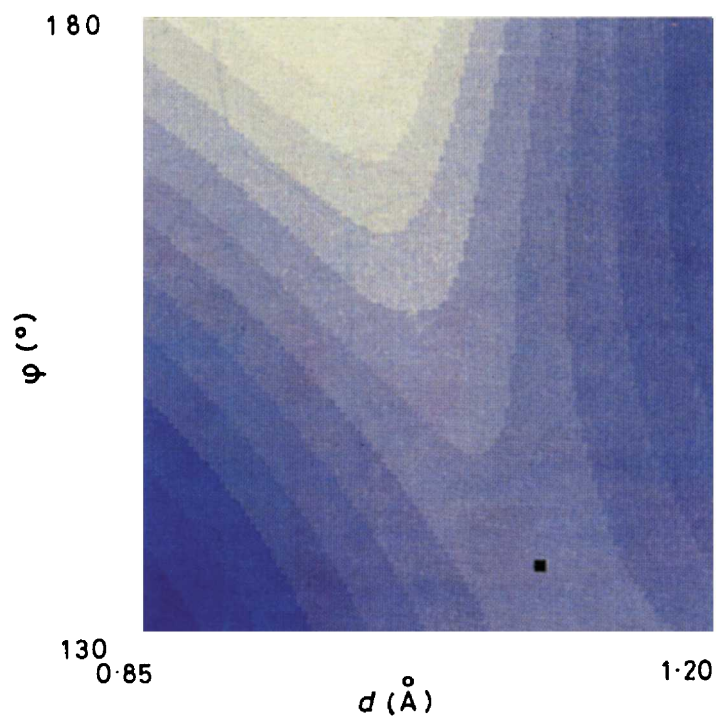


Figure 14. MNDO potential energy contour map for the electrocyclic ring closure of butadiene. Reaction co-ordinates are defined in Figure 4.

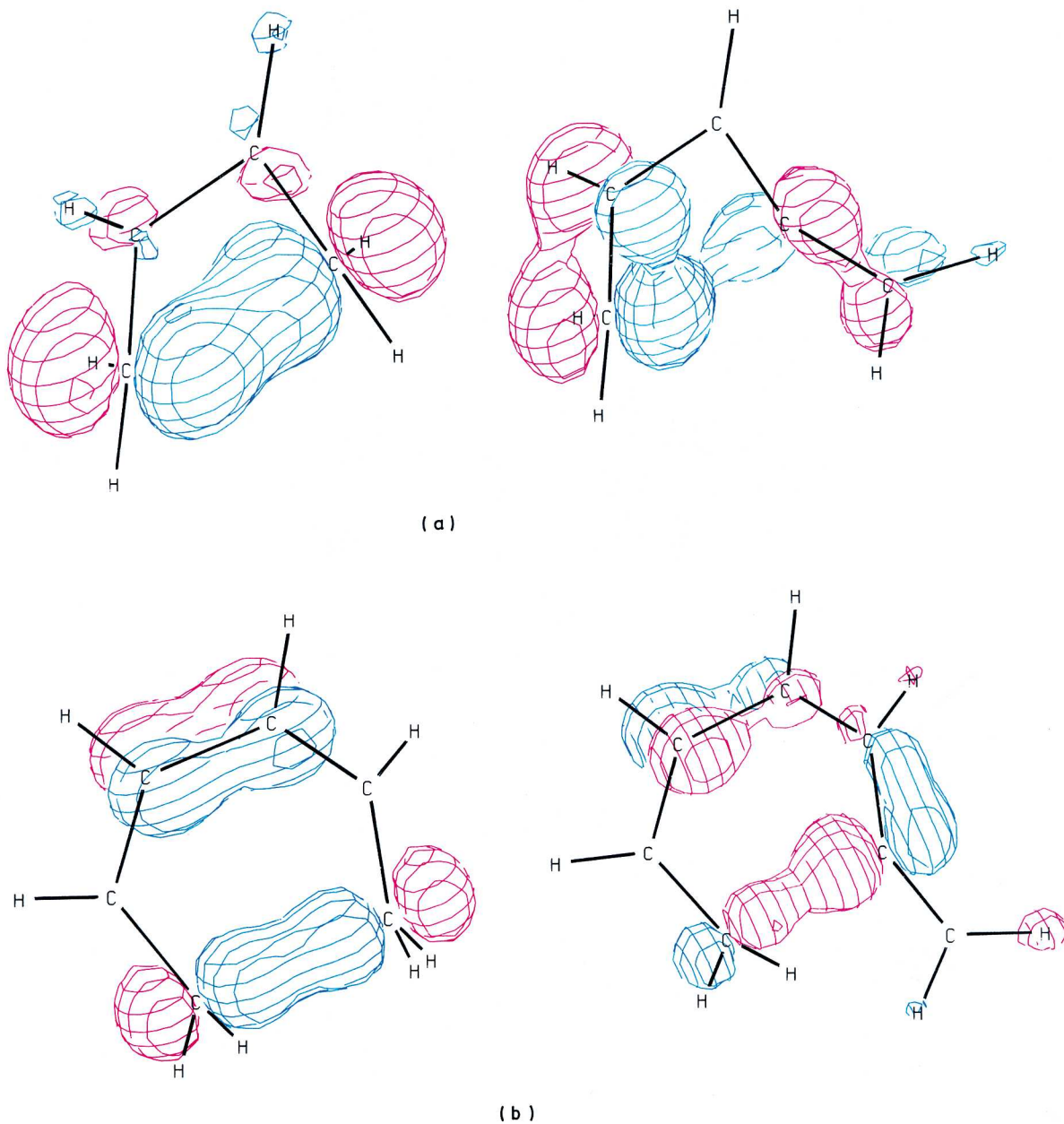


Figure 16. The AM1 HOMO orbital at the transition state for electrocyclicisation of (a) butadiene and (14) and (b) hexa-1,3,5-triene and (15).

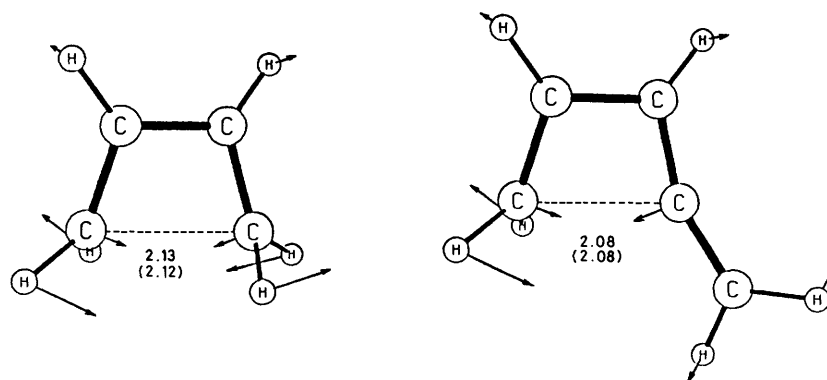


Figure 15. MNDO (AM1) calculated transition state structures for the electrocyclic ring closure of butadiene and (14).

reasons for the lower reactivity of allenes towards dihydrogen reductions seem related to the geometry of the transition states. In the electrocyclic reactions, the geometry of the transition state allows the π system of the alkene component to interact with both the orthogonal π systems of the allene, whereas in the pericyclic dihydrogen transfer, the σ type LUMO of *e.g.* (1) can only interact with one of the two orthogonal π -orbitals of the allene. There is therefore no extra stabilisation of the transition state for dihydrogen transfer.

The Reduction of Cyclopropane by (1).—It is well established that three-membered rings possess unsaturated character similar to that of a double bond. This analogy was manifested in the capacity of cyclopropanes for conjugation with unsaturated groups and their unusual reactivity such as facile metal-catalysed hydrogenation, BF_3 catalysed acetoxylation, inorganic acid ester formation and Markovnikov addition of HX resulting in the opening of the three-membered ring.²⁷ We have investigated the hydrogenation of cyclopropane by (1) (Table 1), a reaction which is known to lead to traces of propane.²⁷ The estimated barriers for the concerted process (99.2 and 73.3 kcal mol⁻¹ by MNDO and AM1, respectively) were prohibitively high, suggesting that this reaction should clearly proceed through a radical pair mechanism. The latter was predicted to occur with an activation energy similar to that of the reduction of ethene by ethane which has been demonstrated to involve radical intermediates.⁹

The Reduction of Substituted π -Bond Systems Containing One or More Heteroatom by (1).—The reduction of formaldehyde was calculated to be significantly higher than for ethene, although the concerted/stepwise balance was virtually unaltered. The higher barrier can be rationalised in simple terms by the greater separation in energy between the σ LUMO on (1) and the π -type HOMO of the carbonyl group compared with ethene. The reduction of the N=N bond in (5) was still higher in energy, but this result is almost certainly an artifact of the AM1 nitrogen parametrisation (see above). Compounds containing double bonds between the heavier main-group elements such as silicon and phosphorus are currently of particular interest.²⁸ A number of molecular orbital calculations at various levels on the substrates themselves have been reported, ranging from EHMO and CNDO to large basis-set correlated *ab initio* methods,²⁸ mainly aimed at elucidating the ground state properties of these systems. Most of the kinetically stabilised disilenes and diphosphenes have been demonstrated to undergo typical addition reactions, some of which are thought to proceed through a radical-chain mechanism.²⁹ Since AM1 parameters have not yet been reported for phosphorus or

silicon, discussion of compounds containing these elements will be based only on the MNDO results.

The calculated barriers for the reduction of the model compounds (16)–(19) (Table 1) were found to be substantially lower compared with those of the analogous reduction of ethene. This can be attributed to the size of the silicon and phosphorus atoms, which dictates the strength and spatial arrangement of the double bond. Thus, the longer distance between the constituent p atomic orbitals not only reduces the effectiveness of the overlapping and, therefore, weakens the π bond, but also geometrically facilitates the interaction with the σ N–H type LUMO of (1). This type of argument may also explain the change in balance in favour of the concerted pathway (*t.s.* 1) for the phosphorus and to a lesser extent the silicon systems (Table 1).

The Reduction of Substituted p -Bond Systems by Other Dihydrogen Donors.—There are several dihydrogen transfer reactions that are known to be initiated by the formation of a radical pair, followed by a radical-chain mechanism. Metzger *et al.* have recently demonstrated that the degenerate dihydrogen exchange between ethane and ethene involves radical intermediates.⁹ In accord with experiment, both semiempirical methods predict significantly lower activation energies for the open-shell route for this specific reaction [Figures 17(a) and (b)]. The MNDO and AM1 absolute barriers for the concerted pericyclic process are 81.2 and 52.4 kcal mol⁻¹ respectively, and are among the highest calculated in this study, clearly because of thermodynamic reasons (Table 2). The value of 71 kcal mol⁻¹ calculated at the correlated multiconfigurational (FORS-MCSCF) *ab initio* level using a double-zeta basis set,⁴ is also prohibitively high for a concerted reaction. Taken together, these results strongly support a non-concerted mechanistic pathway for the reaction of ethane as a dihydrogen donor.

Another factor which constitutes a strong driving force for the reaction is gain of aromaticity as a result of loss of dihydrogen. The extent of aromaticity in the product determines the ease of hydrogenation for both the concerted and radical pair pathways. Thus, the AM1 concerted barrier for cyclohexa-1,3-diene was 11.4 kcal mol⁻¹ lower than ethane, and the value for (3) was very similar to di-imide itself. The difference between the concerted and stepwise routes is also reduced, from 13.4 (ethane) to 7.4 kcal mol⁻¹ (3). Reductions of 'anti-aromatic' species also proceed fairly easily; the barrier to hydrogenation of cyclobutadiene by (1) was found to be 7.1 (MNDO) and 11.8 kcal mol⁻¹ (AM1) lower than ethene for the concerted process. Conversely, when such species are formed in the course of the

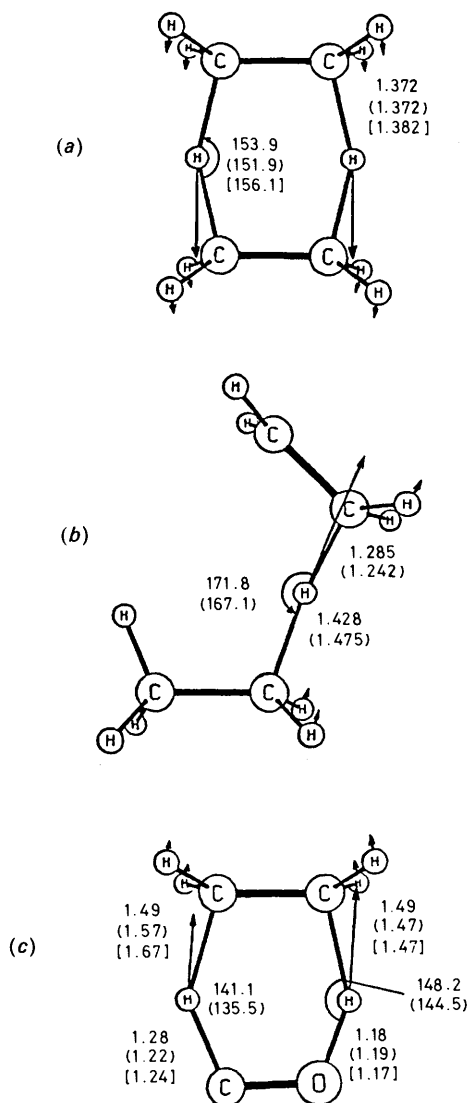


Figure 17. MNDO, (AM1), [3-21G] calculated transition state structures and calculated geometrical parameters for (a) the concerted and (b) stepwise intermolecular dihydrogen exchange between ethane and ethene and (c) the concerted reduction of ethene by (2).

reaction, as in the case of loss of dihydrogen from cyclobutene, there is a substantial increase in the enthalpic barrier.

Hydroxymethylene (2) as a hydrogen donor in the reduction of π systems has been proposed to explain the formation of methanol in the low temperature matrix photolysis of formaldehyde³⁰ and the formation of small amounts of butane during the generation of (2) in the presence of (*Z*)-but-2-ene.² The driving force for this hydrogenation is certainly the formation of carbon monoxide as a reaction product. The AM1 barriers for dihydrogen transfer to ethene by this species (19.4 and 22.2 kcal mol⁻¹ for the concerted and radical-pair mechanisms, respectively) are significantly lower than for (1) as a donor, the former value being in good accord with previous *ab initio* calculations at the uncorrelated SCF level (17.0, 24.3, and 23.7 kcal mol⁻¹ at 3-21G, 6-31G//3-21G and 6-31G**//3-21G basis-set levels).² Interestingly, at the MP2/6-31G**//3-21G level, which includes a first-order correction for electron correlation energy, the barrier for this reaction was found to vanish.² Although this result was obtained with no re-optimisation of geometry at the MP2 level, it nevertheless

suggests that electron correlation may lower the energy of the synchronous concerted pathways of such reactions significantly. It is interesting to note in this context that the AM1 result, which implicitly includes correlation corrections *via* the parametrisation, gives a result which is very similar to the *ab initio* calculations at the uncorrelated SCF level. This is not too surprising, since the AM1 method was almost exclusively parametrised on the basis of the properties of molecules in their equilibrium ground state. The MNDO value for the concerted barrier (53.7) is clearly anomalous. The AM1 and *ab initio*/3-21G calculations predict similar transition state structures, differing significantly only in the estimated length of the developing bond between the ethylenic carbon and the hydroxylic hydrogen atom [Figure 17(c)]. Similar low barriers (10.4 kcal mol⁻¹, STO-3G) have also been reported by other workers for the hydrogenation of formaldehyde by (2).³¹

Formaldehyde is isoelectronic with (4), and surprisingly has never itself been regarded as a potential dihydrogen donor. Calculations (Table 1) revealed quite lower barriers for its reduction of ethene (44.4 and 34.8 kcal mol⁻¹ for the concerted and stepwise process, respectively, at the AM1 level). Such barriers suggest that at relatively high temperatures formaldehyde may transfer dihydrogen to a particularly reactive unsaturated species, rather than eliminate molecular hydrogen to give carbon monoxide *via* a thermally forbidden four-electron process.

Another potentially good dihydrogen donor is the phosphorus analogue (P₂H₂) (19) of di-imide. The MNDO barrier is significantly lower than for (2), although it seems unlikely that (22) could ever be generated with sufficient lifetime to effect dihydrogen reduction.

The Reduction of Substituted π -Bond Systems by Oxy-anion Assisted Dihydrogen Donors.—Significant rate enhancements have been observed for several types of pericyclic process by the use of alkoxide anion substituents. Such substituents decrease the homolytic bond dissociation energy of α C-H and C-C bonds relative to the corresponding OH group (the 'oxy-anion' effect).³² Recent MNDO calculations on the ene reaction have confirmed this trend, corresponding to an oxy-anion-induced weakening of the α C-H bond by approximately 18 kcal mol⁻¹.³³ It was of interest therefore to see if the oxy-anion effect might be utilised in dihydrogen transfer reactions, particularly since the di-anion of *e.g.* (22) would be a readily available reagent. We have calculated the reduction of ethene using as models the species (20)–(23) (Table 2). Whereas the presence of α -hydroxy groups does not affect the rate of the process significantly, alkoxide anion substituents decrease the barrier for the concerted process by either 28.5 (MNDO) or 29.8 (AM1) kcal mol⁻¹. However, the Hessian matrix of these synchronous stationary points displayed two large negative eigenvalues, one of which corresponding to distortion towards a stepwise mechanism (Figure 18). Thus, the asymmetric stationary points now represent the only genuine transition states, and correspond to a hydride transfer to the alkene to form a carbanion together with (following a proton transfer) an enolate anion. The driving force for this pathway is without doubt the separation of charge from the initial di-anion, leading to the conclusion that alkoxy substituents alter the mechanistic nature of dihydrogen transfer reactions, tending towards stepwise mechanisms. The final step, involving the interaction of two negative ions, has a very high calculated barrier (Table 2). It is noteworthy that the lowering of the energy of the (higher order) saddle point for dihydrogen transfer is chiefly effected by the first alkoxide anion (21), the second one (23) being essentially of minor importance to the energetics of the process (Table 2). Since the separation of negative charge (in the gas phase model as used here) is at least partially responsible for these character-

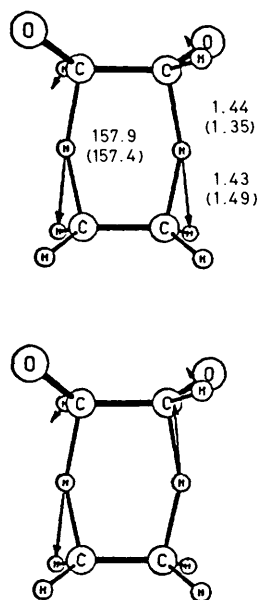


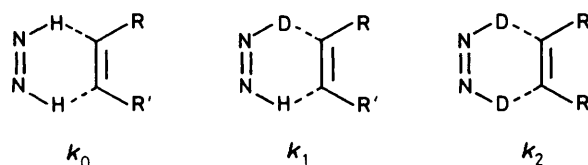
Figure 18. MNDO (AM1) calculated displacement vectors corresponding to the two large imaginary frequencies calculated from the Hessian matrix, for the concerted second-order saddle point of the reaction of (23) with ethene.

Table 5. Thermodynamic properties for the concerted and stepwise mechanisms for selected (1) reductions, at 300 K.

		1		2	
		MNDO	AM1	MNDO	AM1
Ethene	ΔS^\ddagger	-39.89	-39.71	-27.26	-26.48
	ΔG^\ddagger	66.7	44.2	51.8	40.7
Ethyne	ΔS^\ddagger	-34.78	-34.69	-23.91	-22.47
	ΔG^\ddagger	68.0	47.2	55.3	45.0
Dicyanoethyne	ΔS^\ddagger	-35.16	-35.29	-21.69	-20.57
	ΔG^\ddagger	72.4	47.4	54.2	39.2
Cyclopropene	ΔS^\ddagger	-39.38	-39.44	-29.25	-26.99
	ΔG^\ddagger	61.9	36.8	54.3	34.5
Cyclobutene	ΔS^\ddagger	-39.74	-39.54	-30.54	-27.68
	ΔG^\ddagger	66.2	39.4	49.5	37.0
<i>cis</i> -But-2-ene	ΔS^\ddagger	-44.26	-44.71	-31.75	-31.83
	ΔG^\ddagger	74.8	49.6	56.2	44.6
<i>trans</i> -But-2-ene	ΔS^\ddagger	-44.50	-43.34	-31.22	-30.24
	ΔG^\ddagger	74.6	49.6	55.8	44.6
(8)	ΔS^\ddagger	-40.23	-40.67	-35.60 ^a	-33.73
	ΔG^\ddagger	51.0	21.2	-34.07 ^b	-33.17
Methylene-cyclopropene	ΔS^\ddagger	-39.29	-39.15	41.2 ^a	24.3
	ΔG^\ddagger	70.0	45.8	29.2 ^b	16.2
Benzynes	ΔS^\ddagger	-38.58		-27.24 ^c	-26.26
	ΔG^\ddagger	28.0		-29.41 ^d	-27.24
(5)	ΔS^\ddagger	-38.63	-34.34	52.9 ^c	42.0
	ΔG^\ddagger	89.0	74.7	55.5 ^d	42.8

^a Via the tertiary bicyclic radical. ^b Via the secondary bicyclic radical. ^c Via the tertiary radical. ^d Via the primary radical. Entropies in kcal mol⁻¹, Gibbs free energies in cal mol⁻¹ K⁻¹.

istics, we decided to model a more solution-like environment by introducing point charge counter ions. As is expected, the 'oxy-anion' effect is attenuated by the introduction of such point charges, or 'sparkles,' which represent unipositive and dipositive



Scheme 2.

hard-spheres with ionic radius 0.7 Å (the positions of which were fully optimised with respect to the oxygen atoms), but the basic characteristics of the potential surface were not altered. It seems unlikely therefore that oxy-anion substituents could be used for inducing stereoselective dihydrogen transfers. We also investigated 1,2-difluoroethane as a hydrogen donor, since it is formally isoelectronic to (23). The concerted barrier is little different from that for ethane itself, revealing a very small α -fluorine effect. The stepwise pathway is reduced in energy however, due to stabilisation of the intermediate radical by the α -fluorine substituent.

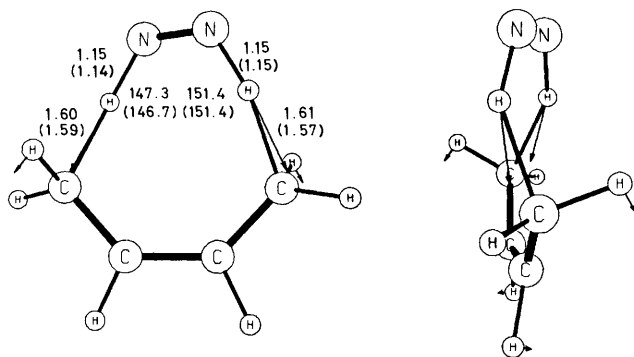
Thermodynamic Properties.—There is a relatively greater loss of degrees of freedom at the transition state for synchronous dihydrogen transfer compared with the stepwise process, which may play a significant role in the balance between the two mechanisms. To test this hypothesis, ΔS^\ddagger and ΔG^\ddagger were calculated for several reactions with (1) as the donor at 300 K (Table 5). The calculated activation entropies for the concerted pathway (*t.s.* 1) appeared uncorrelated with the magnitude of ΔG^\ddagger for the reaction. For example, ΔS^\ddagger for ethene and (5) are quite similar. The most significant effect was for *cis*- and *trans*-but-2-ene, where ΔS^\ddagger was significantly more negative than the majority of reactions, probably as a result of the loss of rotational degrees of freedom for the methyl groups in the relatively tight transition state. This restriction in the rotational freedom is more severe for the *cis*-alkene and results in raising the relative free energy of activation (with the exception of the MNDO concerted pathway) rendering the two mechanisms equally probable at the AM1 level. The entropy of activation for *t.s.* 1 was normally between 6–15 cal mol⁻¹ K⁻¹ more negative than for *t.s.* 2, corresponding to a difference of 2–5 kcal mol⁻¹ in ΔG^\ddagger in favour of the stepwise mechanism. This difference however did appear related to the magnitude of ΔG^\ddagger , the reactions with a low enthalpic barrier showing a smaller difference in ΔS^\ddagger than those with higher barriers.

Hydrogen Kinetic Isotope Effects.—The two possible mechanistic pathways for dihydrogen reductions differ most conspicuously in the degree of hydrogen motion present in the transition states. We wished to establish whether the primary hydrogen isotope effects for the concerted route could be related to the symmetry and properties of the transition state, the relationship between the isotope effects for mono (k_0/k_1) or di-substitution (k_0/k_2) of deuterium on (1), and the differences between the concerted and stepwise routes. Calculated isotope effects for the concerted pathway (*t.s.* 1) for both d_1 and d_2 substitution on (1) and that for the stepwise pathway (*t.s.* 2) for mono-deuterium substitution on the *transferring* hydrogen are shown in Table 6. The results show that k_0/k_1 for the concerted pathway is significantly lower than that expected for a purely three-centre hydrogen movement such as found in *e.g.* simple proton transfers, whilst k_0/k_2 is significantly higher. The relationship between the two isotope effects follows a geometric rule, *i.e.* $(k_0/k_2)^{0.5} = (k_0/k_1)$, very closely in all the systems studied, which suggests that the observation of such a relationship experimentally would be a good indication of a concerted mechanism. The magnitude of the isotope effects is surprisingly

Table 6. Kinetic isotope effects for selected dihydrogen transfers at 298 K.

	Concerted		Stepwise	
	MNDO	AM1	MNDO	AM1
Ethene	3.252 ^a 11.847 ^b	3.259 11.791	7.221 9.279	6.805 8.736
Cyclopropene	3.090 ^a 10.533 ^b	3.033 10.096	7.073 8.657	6.421 7.823
Cyclobutene	3.159 ^a 11.102 ^b	3.093 10.577	7.014 8.732	6.592 8.191
Cyclobutadiene	3.136 ^a 10.877 ^b	2.958 9.565	5.700 5.502	6.407 7.805
Ethyne	3.186 ^a 11.352 ^b	3.392 12.689	7.773 10.05	7.167 9.273
1,2-Dicyanoethyne	3.258 ^a 11.858 ^b	3.420 12.555	7.501 9.684	6.867 8.741
(5)	3.036 ^a 11.403 ^b	3.729 17.007	6.512 8.518	6.208 7.862
Methylenecyclopropene	3.195 ^a 11.483 ^b	3.196 11.034	7.282 ^c 9.357 ^c	6.813 8.728
		<i>a</i>	6.988 ^d	6.511
		<i>b</i>	8.865 ^d	8.246
Benzynes	2.432 ^a 6.047 ^b		7.317 8.179	5.290 5.773
(8)	2.598 ^{a,e} 3.228 ^{a,f} 9.082 ^b	2.244 2.980 6.851	7.005 ^g 1.145 ^g 8.110 ^g 6.953 ^{a,e,h} 1.184 ^{a,f,h} 8.331 ^{b,h}	6.673 1.142 7.616 6.577 1.185 7.792

^a Harmonic rate ratios for N₂HD. ^b Harmonic rate ratios for N₂D₂. ^c Via the tertiary radical. ^d Via the primary radical. ^e Deuterium delivered to C-2. ^f Deuterium delivered to C-1. ^g Via the secondary bicyclic radical. ^h Via the tertiary bicyclic radical.

**Figure 19.** Two views for the MNDO (AM1) calculated transition state structures for the 1,4-antarafacial reduction of butadiene by (1).

invariant to minor changes in the transition state structures (Table 6), although major effects are seen for very early transition states involving *e.g.* benzyne or (8). In these systems the zero-point energy differences between reactant and transition state are smaller, and significantly smaller isotope effects are predicted. Nevertheless, the geometric rule is still closely followed. In the stepwise pathway, only one hydrogen is directly involved in the transition state (*t.s.* 2), and the predicted isotope effects are noticeably lower than for the concerted route, although the differences are not so great that an unambiguous experimental distinction between the two mechanisms could be easily made on this basis. The most unexpected effect was for benzyne [and to a lesser extent (8)], where the isotope effect for *d*₂ transfer was actually higher for the stepwise route, emphasising the difficulty of a direct comparison of three-centre and six-centre isotope effects.

1,4-Dihydrogen Reduction of Butadiene by (1).—Besides the normal 1,2-addition to isolated unsaturated bonds, (1) could in principle transfer dihydrogen antarafacially *via* a 1,4-addition to a conjugated diene. Although only traces of the 1,4-addition product, but-2-ene, have been detected in the gas phase reduction of butadiene,^{1c} we chose to investigate this reaction to establish whether secondary orbital effects might exert any significant influence on the process. The calculations on the 1,4-hydrogenation of butadiene (Figure 19) predict an AM1 activation energy for the synchronous pathway of no less than 70.3 kcal mol⁻¹ which is consistent with the experimentally manifested reactivity. The open-shell route, although being energetically a reasonable alternative, would be largely determined by topological factors which seem to favour a fast disproportionation towards the 1,2-product. Whereas the geometries of the transition states do not allow interaction between the orthogonal π system of allenes and the LUMO of (1), these geometric constraints no longer hold in the transition states involved in the 1,4-processes. Here the orthogonal π system is more favourably orientated towards the migrating hydrogens, strongly suggesting the possibility of a significant lowering of the activation energy for such reductions. The species (24) possesses two orthogonal π systems at both termini of the diene framework and would therefore be expected to exhibit a maximal secondary orbital effect for 1,4-hydrogen addition. The semiempirical results confirmed this prediction; the concerted 1,4-antarafacial addition to (24) was found to require an activation energy of 84.8/60.1 kcal mol⁻¹ (MNDO/AM1), values that are 13.3/10.2 (MNDO/AM1) less than for butadiene. Although the alternative 1,2-reaction of (24) has a slightly higher barrier than the reduction of ethene, it still remains the favoured process by a wide margin.

1,2-Dimethyl Transfer to Ethene by (25).—Unlike the well manifested reactivity of (1) as a reducing agent, no examples seem to exist for the analogous process involving methyl rather than hydrogen transfer from *cis*-azomethane (25) to an unsaturated bond. *cis*-(25) is a known, well characterised and relatively thermally stable species, which can be prepared either by photoisomerisation of the *trans* form³⁴ or by a retrograde Diels-Alder reaction.³⁵ We have extended our calculations to the (25)/ethene system, since several aspects of this transformation are of special theoretical interest. Indeed, orbital symmetry considerations suggest that the reaction could, *a priori*, take place with either inversion or retention of configuration at both the migrating centres. At the closed-shell RHF level, the symmetric stationary points corresponding to a synchronous transfer of the two methyl groups with either retention or inversion of configuration both displayed *two* negative roots in the calculated second derivative matrix, the minor one corresponding to an asymmetric distortion. This result was in fact expected on the basis of the known deficiencies of the AM1 nitrogen parametrisation, since the system involves the concurrent cleavage of two C-N bonds in the transition state. As mentioned in previous sections, the inaccuracies of the CRF are particularly acute for C-N bond formation processes (*e.g.* cycloaddition reactions¹⁹) and they often result in qualitative changes in the potential surface. It is therefore rather unlikely that the extra imaginary frequencies carry any chemical significance. Although the symmetric stationary points were not genuine transition states, the estimated activation energies reveal an unambiguous trend in favour of the double-inversion process (Table 2) which, under certain considerations, could be realistic. Dimethyl transfer with double-inversion was found to require 12.2 or 27.3 kcal mol⁻¹ less than the double-retention route at the MNDO and AM1 levels, respectively. The greater AM1 energy difference between the two pathways probably reflects the enhanced steric hindrance imposed

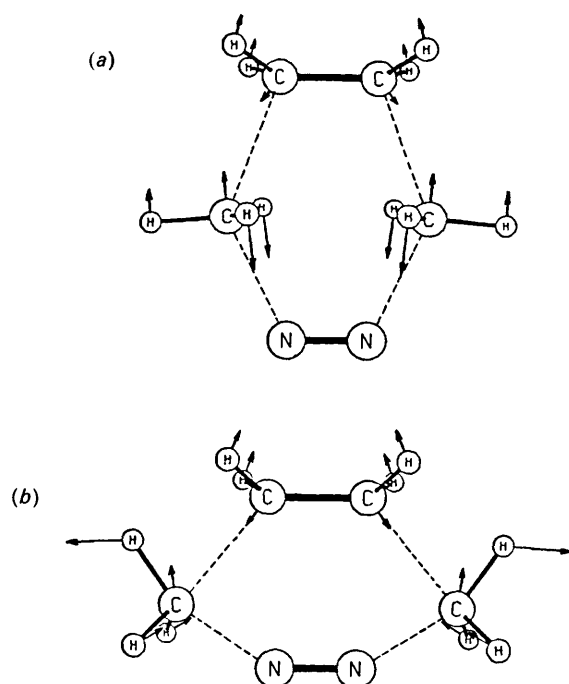


Figure 20. Transition states for the concerted dimethyl transfer to ethene by (25), with (a) inversion and (b) retention of configuration at the migrating centre.

on the transition state for inversion (Figure 20) which is incorrectly overestimated at the MNDO level. This additional steric repulsion and the entropic consequences following the restriction on the rotational freedom of the methyl groups, seem to be largely compensated by the efficiency with which the frontier orbitals are allowed to overlap in the transition state. Indeed, while both phases of the $2p_x$ orbitals of the migrating carbons are utilised in the HOMO-LUMO interaction in the activated complex for inversion, this enhanced stabilising overlap cannot be achieved *via* the retention route. The latter becomes even more disfavoured by the continuous accumulation of angle strain on the migrating carbons as the system approaches the transition state. Although these arguments provide a satisfactory explanation of the predicted preference for double inversion, it should be noted that the transition states for the two routes differ markedly in their geometric characteristics. The N-C/C-C bond lengths and N-C-C angle of migration are $1.85 \text{ \AA}/2.15 \text{ \AA}/81.2^\circ$ for retention and $1.87 \text{ \AA}/2.05 \text{ \AA}/138.2^\circ$ for inversion, respectively, implying that improvement of the core repulsion function might not equally affect the activation energies for the two alternative pathways. This possibility is reinforced by the effect which the revised core repulsion function had on the barriers for the two processes. Whereas the barrier for inversion was reduced by $26.9 \text{ kcal mol}^{-1}$ when the new nitrogen parameter was employed, that for retention was only affected by $15.2 \text{ kcal mol}^{-1}$, both synchronous transfers still corresponding to second-order saddle points. Since the new nitrogen Gaussian parameter does not correspond to a rigorous solution to the CRF problem, it appears difficult to estimate the real difference in the enthalpic requirements for the two routes. Furthermore, it seems unlikely that synchronous transfer of two methyl groups will ever be observed experimentally, since the estimated absolute semi-empirical barriers were prohibitively high (153.6 and $126.3 \text{ kcal mol}^{-1}$ for retention and inversion, respectively). However, these barriers as well as the balance between the two mechanisms could be very sensitive to geometric factors, more so than the di-imide analogue. The barriers to the stepwise pathways for

retention and inversion were lower by 49.0 and $55.8 \text{ kcal mol}^{-1}$ than the corresponding concerted routes, suggesting that the reaction would almost certainly proceed *via* a radical pair mechanism. The preference for migration with double-inversion is even more conspicuous for the open-shell route (Table 2), since severe steric hindrance can be avoided and ideal orbital disposition can be achieved in the essentially linear transition state for inversion. The relatively large estimated barriers for the disproportionation of the intermediate radical pairs (53.8 and $17.5 \text{ kcal mol}^{-1}$ for retention and inversion, respectively) suggest that dimethyl transfers may not be stereospecific reactions.

Acknowledgements

We wish to thank the University of London for a grant of time on the FPS-164 system at Imperial College. One of us (D. A.) thanks the A. Onassis Foundation for financial support.

References

- 1 E. E. van Tamelen, R. S. Dewey, M. F. Lease, and W. H. Pirkle, *J. Am. Chem. Soc.*, 1961, **83**, 4302; S. Hunig, H. R. Muller, and W. Thier, *Angew. Chem., Int. Ed. Engl.*, 1965, **4**, 271; S. K. Vidyarthi, C. Willis, R. A. Back, and R. M. McKittrick, *ibid.*, 1974, **96**, 7647; C. Willis, R. A. Back, J. M. Parsons, and J. G. Purdon, *J. Am. Chem. Soc.*, 1977, **99**, 4451.
- 2 S. N. Ahmed, M. L. McKee, and P. B. Shevlin, *J. Am. Chem. Soc.*, 1985, **107**, 1320.
- 3 W. V. E. Doering and J. W. Rosenthal, *J. Am. Chem. Soc.*, 1967, **89**, 4534.
- 4 D. F. Feller, M. W. Schmidt, and K. Ruedenberg, *J. Am. Chem. Soc.*, 1982, **104**, 960.
- 5 H. S. Rzepa and J. Miller, *J. Chem. Soc., Perkin Trans. 2*, 1985, 717; M. L. McKee, P. B. Shevlin, and H. S. Rzepa, *J. Am. Chem. Soc.*, 1986, **108**, 5793.
- 6 P. N. Skancke, *Chem. Phys. Lett.*, 1977, **47**, 259; D. J. Pasto and D. M. Chipman, *J. Am. Chem. Soc.*, 1979, **101**, 2290.
- 7 For a preliminary report, see, D. K. Agrafiotis and H. S. Rzepa, *J. Chem. Soc., Chem. Commun.*, 1987, 902.
- 8 M. J. S. Dewar, *J. Am. Chem. Soc.*, 1984, **106**, 209; M. J. S. Dewar, S. Olivella, and J. J. P. Stewart, *ibid.*, 1986, **108**, 5771.
- 9 D. Malwitz and J. O. Metzger, *Angew. Chem., Int. Ed. Engl.*, 1986, **25**, 762; J. O. Metzger, *ibid.*, 1974, **96**, 7647.
- 10 For the theoretical background to the MNDO method, see, M. J. S. Dewar and W. J. Thiel, *J. Am. Chem. Soc.*, 1977, **99**, 4899; *Theor. Chim. Acta*, 1977, **46**, 89; *Quantum Chemistry Program Exchange*, Program No. 506, Bloomington, Indiana, U.S.A.
- 11 We are grateful to Dr J. McKelvey, Eastman Kodak, Rochester, for providing us with a copy of his ROHF program. For other open-shell solutions, see M. J. S. Dewar and S. Olivella, *J. Chem. Soc., Faraday Trans.*, 1979, **75**, 829.
- 12 S. B. Brown, M. J. S. Dewar, G. P. Ford, D. J. Nelson, and H. S. Rzepa, *J. Am. Chem. Soc.*, 1978, **100**, 7832; H. S. Rzepa, *J. Chem. Soc., Chem. Commun.*, 1981, 939; B. Anhede, N. A. Bergman, and L. Melander, *Acta Chem. Scand., Ser. A*, 1983, **37**, 843; J. P. Shea, S. D. Nelson, and G. P. Ford, *J. Am. Chem. Soc.*, 1983, **105**, 5451.
- 13 W. L. Jorgensen, *Quantum Chemistry Program Exchange*, 1983, **15**, 340.
- 14 D. K. Agrafiotis and H. S. Rzepa, ICTOS (Imperial College Theoretical Organic Software) Program System, Imperial College, 1988.
- 15 C. Willis and R. A. Back, *Can. J. Chem.*, 1973, **51**, 3605; R. A. Back, C. Willis, and D. A. Ramsay, *ibid.*, 1974, **52**, 1006.
- 16 J. Baker, University of Cambridge, personal communication.
- 17 M. J. S. Dewar and D. M. Storch, *J. Am. Chem. Soc.*, 1985, **107**, 3898.
- 18 M. J. S. Dewar, E. G. Zoebisch, E. F. Healy, and J. J. P. Stewart, *J. Am. Chem. Soc.*, 1985, **107**, 3902.
- 19 L. Grierson, M. J. Perkins, and H. S. Rzepa, *J. Chem. Soc., Chem. Commun.*, 1987, 1779.
- 20 H. S. Rzepa, *J. Chem. Res. (S)*, 1988, 224.
- 21 R. W. Fessenden, *J. Phys. Chem.*, 1964, **68**, 1508.
- 22 K. M. Merz and C. H. Reynolds, *J. Chem. Soc., Chem. Commun.*, 1988, 90.

- 23 M. J. S. Dewar, G. P. Ford, and H. S. Rzepa, *J. Mol. Struct.*, 1979, **51**, 275.
- 24 R. T. Seidner, N. Nakatsuka, and S. Masamune, *Can. J. Chem.*, 1970, **48**, 187.
- 25 P. J. Dunn and H. S. Rzepa, *J. Chem. Soc., Perkin Trans. 2*, 1987, 1669.
- 26 J. S. Burnier and W. L. Jorgensen, *J. Org. Chem.*, 1984, **49**, 3001; H. M. Saxton, J. K. Sutherland, and C. Whaley, *J. Chem. Soc., Chem. Commun.*, 1987, 1449.
- 27 For a review, see Lukina, *Russ. Chem. Rev.*, 1962, **31**, 419.
- 28 A. H. Cowley, *Polyhedron*, 1984, **3**, 389; R. West, *Science*, 1984, **225**, 1109.
- 29 S. Masamune, Y. Hanzawa, S. Murakami, T. Bally, and F. J. Blount, *J. Am. Chem. Soc.*, 1982, **104**, 1150.
- 30 J. R. Sodeau and E. K. C. Lee, *Chem. Phys. Lett.*, 1978, **57**, 71.
- 31 M. J. H. Kemper, C. H. Hoeks, and H. M. Buck, *J. Chem. Phys.*, 1981, **74**, 5744.
- 32 M. L. Steigerwald, W. A. Goddard, and D. A. Evans, *J. Am. Chem. Soc.*, 1979, **101**, 1994.
- 33 I. G. El Karim and H. S. Rzepa, *J. Chem. Soc., Chem. Commun.*, 1987, 193.
- 34 G. S. Hartley, *Nature (London)*, 1937, **140**, 281; A. H. Cook, *J. Chem. Soc.*, 1938, 876; *ibid.*, 1939, 1309; E. R. Talaty and J. C. Fargo, *J. Chem. Soc., Chem. Commun.*, 1967, 65; E. V. Brown and R. Granneman, *J. Am. Chem. Soc.*, 1975, **97**, 621.
- 35 S. F. Nelsen, *J. Am. Chem. Soc.*, 1974, **96**, 5669.

Received 14th April 1988; Paper 8/01486H